

2020

## Topical Photodynamic Therapy Generates Microvesicle Particles

Oladayo Ayobami Oyebanji  
*Wright State University*

Follow this and additional works at: [https://corescholar.libraries.wright.edu/etd\\_all](https://corescholar.libraries.wright.edu/etd_all)



Part of the [Pharmacology, Toxicology and Environmental Health Commons](#)

---

### Repository Citation

Oyebanji, Oladayo Ayobami, "Topical Photodynamic Therapy Generates Microvesicle Particles" (2020).  
*Browse all Theses and Dissertations*. 2333.  
[https://corescholar.libraries.wright.edu/etd\\_all/2333](https://corescholar.libraries.wright.edu/etd_all/2333)

This Thesis is brought to you for free and open access by the Theses and Dissertations at CORE Scholar. It has been accepted for inclusion in Browse all Theses and Dissertations by an authorized administrator of CORE Scholar. For more information, please contact [library-corescholar@wright.edu](mailto:library-corescholar@wright.edu).

# Topical Photodynamic Therapy Generates Microvesicle Particles

A Thesis submitted in partial fulfillment  
of the requirements for the degree of  
Master of Science

by

Oladayo Ayobami Oyebanji  
MBChB, Obafemi Awolowo University  
Nigeria, 2014

2020  
Wright State University

Wright State University  
GRADUATE SCHOOL

April 24, 2020

I HEREBY RECOMMEND THAT THE THESIS PREPARED UNDER MY SUPERVISION BY Oladayo Ayobami Oyebanji ENTITLED Topical Photodynamic Therapy Generates Microvesicle Particles BE ACCEPTED IN PARTIAL FULFILLMENT OF THE REQUIREMENTS FOR THE DEGREE OF Master of Science.

---

Jeffrey B. Travers, M.D., Ph.D.  
Thesis Director

---

Jeffrey B. Travers, M.D., Ph.D.  
Chair, Department of Pharmacology and Toxicology

Committee on  
Final Examination

---

Jeffery B. Travers, M.D., Ph.D.

---

Ravi P. Sahu, Ph. D.

---

Ji C. Bihl, M.D., Ph.D.

---

Barry Milligan, Ph.D.  
Interim Dean of the Graduate School

## ABSTRACT

Oyebanji, Oladayo Ayobami. M.S., Department of Pharmacology and Toxicology, Wright State University, 2020. *Topical Photodynamic Therapy Generates Microvesicle Particles* .

Photodynamic therapy (PDT) involves the use of light at an appropriate wavelength acting on a photosensitizing chemical to cause cell death via generation of reactive oxygen species. PDT has been useful in the management of skin conditions (like acne, psoriasis) and cancers like superficial skin, esophageal and non-small cell lung cancers. In addition to these therapeutic effects, previous murine studies from our group have demonstrated that topical PDT induces immunosuppression in vivo. Thus, topical PDT of skin can generate systemic effects through unknown mechanisms. Our group showed that PDT induces an immunosuppressive effect which occurs partly via Platelet-Activating Factor Receptor (PAFR) signaling. Of importance, PAFR signaling can generate Microvesicle particles (MVP). MVPs are small extracellular membrane-enclosed particles believed to mediate cell-to-cell communication via the transport of bioactive signaling substances. The present studies tested if PDT could generate MVP release. Our studies used in vitro, ex vivo (human skin explants) and in vivo (murine) models. PDT increased MVP release across the different cell lines tested in vitro as well as treatment of human skin explants ex vivo. Murine studies also revealed a significant increase in MVP levels in skin and blood following PDT treatment. We also found a limited role for PAFR in this PDT-generated MVP release. These studies reveal a consistent production of MVPs following PDT and thus, provide insights into a possible novel mechanism whereby PDT exerts systemic effects via the generation of MVPs.

# Contents

<b>1</b>	<b>Introduction</b>	<b>1</b>
1.1	Statement of problem	1
1.2	Significance	1
1.3	Statement of Purpose	1
1.4	Hypothesis	2
1.5	Research objectives	2
1.6	Definitions	2
1.7	Assumptions	4
<b>2</b>	<b>Literature Review</b>	<b>5</b>
2.1	Photodynamic therapy	5
2.1.1	Photochemical reactions in PDT	6
2.1.2	Photosensitizers	7
2.1.3	Applications of PDT	9
2.2	Microvesicle Particles	9
2.3	Platelet Activating Factor Receptor	11
<b>3</b>	<b>Materials and Methods</b>	<b>12</b>
3.1	Introduction	12
3.2	Cell Culture	12
3.2.1	Cell Growth Media and Storage Condition	13
3.2.2	Cell Passage	13
3.2.3	Changing Media	13
3.2.4	Cell Counts	14
3.2.5	Bringing Up Cells from Liquid Nitrogen	14
3.2.6	Treatments	14
3.2.7	Inhibitors	15
3.2.8	MVP Isolation	15
3.2.9	MVP Analysis	15
3.3	MTT Assay for Cell Survival	16
3.4	Skin	16
3.4.1	Treatment	16

3.4.2	Punch Biopsies . . . . .	17
3.4.3	MVP Extraction from Punch Biopsies . . . . .	17
3.5	Mice . . . . .	17
3.5.1	Treatment . . . . .	17
3.5.2	Murine Punch Biopsies . . . . .	18
3.5.3	Blood Sample Collection . . . . .	18
3.6	Statistical Analysis . . . . .	19
<b>4</b>	<b>Results</b>	<b>20</b>
4.1	Generations of MVPs following PDT . . . . .	20
4.1.1	PDT Dose Response in HaCaT Cells . . . . .	20
4.1.2	Time Response in MVP Generation following PDT . . . . .	20
4.1.3	Generation of PDT Across Different Cell Lines . . . . .	24
4.1.4	Generation of MVP following PDT ex vivo . . . . .	24
4.1.5	Generation of MVPs following PDT in vivo . . . . .	24
4.2	Role of Reactive Oxygen Species in the Generation of MVPs following PDT . . . . .	24
4.3	Roles of aSMase in the Generation of MVP following PDT . . . . .	27
4.3.1	Roles of aSMase in the Generation of MVP following PDT in cells . . . . .	29
4.3.2	Role of aSMase in PDT-generated MVP in Skin . . . . .	29
4.3.3	Role of aSMase in PDT-generated MVP in mice . . . . .	29
4.4	Role of Platelet Activating Factor Receptor (PAFR) in PDT-generated MVP . . . . .	33
4.4.1	Role of PAFR in PDT-generated MVP <i>in vitro</i> . . . . .	33
4.4.2	Role of PAFR in PDT-generated MVP in vivo . . . . .	33
<b>5</b>	<b>Discussion</b>	<b>35</b>
5.1	Summary . . . . .	35
5.2	Limitations and Future Studies . . . . .	37
5.3	Conclusion . . . . .	38
<b>6</b>	<b>Appendix</b>	<b>39</b>
6.1	Appendix 1: Supplemental Figures . . . . .	39
6.2	Appendix 2: Procedural Pictures . . . . .	44
	<b>References</b>	<b>46</b>

# List of Figures

2.1	Overview of photochemical reactions during PDT. Several types of primary and secondary photochemical reactions cause production of reactive oxygen species and dose-dependent cellular damage. $H_2O_2$ , hydrogen peroxide; $O_2 (^1\Delta_g)$ , singlet oxygen (excited state); $O_2 (^3\Sigma_g^-)$ , triplet oxygen (ground state); $O_2^-$ , superoxide anion; $OH^\cdot$ , hydroxyl radical; SOD, superoxide dismutase; $X^{-/+}$ , anion/cation species; $X^\cdot$ , radical species. Adapted from ref ([88]) . . . . .	7
2.2	Biosynthesis of heme in mammals. Mitochondrial enzymes are in green while cytosolic enzymes are in red. Adapted from ref [8] . . . . .	8
2.3	Schematic representation of the mechanisms of formation of microvesicles, exosomes and apoptotic bodies ([66]) . . . . .	10
4.1	Dose response curve of PDT-induced MVP release in HaCaT cells. Cells either received No treatment (NT), 500ng PMA in 3mL HBSS+BSA, 100ng CPAF in 3mL HBSS+BSA, 2.5J PDT (208secs), 5J PDT (416secs), 10J PDT (832secs) or 20J PDT (1663secs). PMA and CPAF being positive controls generated 2-3 folds of MVP as compared to control. A progressive increase in MVP count was obtained as PDT dose increased, reaching a peak at 20J. The data depicted are mean SE fold change in MVP count (average of n=3). Groups were compared using one-way ANOVA and Tukey's post-hoc test. Differences in samples were considered significant if the P value was less than 0.05. P<0.05 (*), P<0.01(**), P<0.001(***) and P<0.0001(****). . . . .	21
4.2	Relative survival rate of HaCaT cells following PDT treatment. After the different treatments in Fig. 4, cells were subjected to an MTT assay at 4hours post-treatment. A progressive decline in cell survival rate was seen as PDT dose increased, reaching the lowest at 20J suggesting the most lethal effect on cells. The data depicted are mean SE fold change in MVP count (average of n=3). Groups were compared using one-way ANOVA and Tukey's post-hoc test. Differences in samples were considered significant if P value is less than 0.05. P<0.001(***) and P<0.0001(****). . . . .	22

- 4.3 Time response of PDT-induced MVP production in HaCaT cells. After PDT treatment, supernatants were either harvested immediately (0h) or incubated for 2h, 4h, 8h or 24h before being collected for MVP isolation. A somewhat progressive increase occurred in MVP count as time progresses. There was, however, no significant difference between the count at 4h, 8h and 24h. The data depicted are mean SE fold change in MVP count (average of n=3). Groups were compared using one-way ANOVA and Tukey's post-hoc test. Differences in samples were considered significant if P is less than 0.05. P<0.05 (\*), while ns denotes no significance. . . . . 23
- 4.4 PDT generates MVPs across different cell types. HaCaT (a) NTERT (b) and Fibroblasts (c) were either treated with plain HbSS+BSA (NT), 0.1% EtOH (Veh), 1mM 5ALA, 500ng PMA, 100ng CPAF, Blue light alone (BL) or PDT and were incubated for 4hours. PDT generated significantly high amounts of MVPs across the 3 different cell lines. The data depicted are mean SE fold change in MVP count (average of n=8). Groups were compared using one-way ANOVA and Tukey's post-hoc test. Differences in samples were considered significant if P is less than 0.05. P<0.05 (\*), P<0.01(\*\*), P<0.001(\*\*\*) and P<0.0001(\*\*\*\*). . . . . 25
- 4.5 PDT generates MVPs ex vivo in human skin. Human skin explants were treated with nothing (NT), 90% DMSO in 10% EtOH, 100ng 5ALA, 500g PMA in 100L DMSO, 250g CPAF in 100L DMSO, Blue light alone (BL) or PDT and were incubated for 4hours at 37C after which biopsies were taken. PDT generated significant amount of MVP. The data depicted are mean + SE fold change in MVP count (average of n=5). Groups were compared using one-way ANOVA and Tukey's post-hoc test. Differences in samples were considered significant if P is less than 0.05. P<0.05 (\*) and P<0.01(\*\*). . . . . 26
- 4.6 PDT generates MVPs in vivo in Mice skin. C57BL6 mice had their backs shaved and were treated with 90% DMSO (Sham), 500g PMA, or PDT. Biopsies and blood samples were taken after 4hours. PDT generated significant amount of MVP both in skin (a) and plasma (b). The data depicted are mean SE fold change in MVP count (data was from at least n=5mice). Groups were compared using one-way ANOVA and Tukey's post-hoc test. Differences in samples were considered significant if P is less than 0.05. P<0.001(\*\*\*) . . . . . 27



- 4.7 Antioxidants inhibit production of MVPs by PDT in vitro. HaCaT cells had 5-ALA incubation in the dark for 4hrs and were then treated with the antioxidants, 0.5mM Vitamin C (VitC) and 0.5mM N-acetylcysteine (NAC) for 1hour. Cells were subsequently exposed to blue light and supernatant were harvested 4hrs later. Other groups were treated as earlier described. Both antioxidants significantly reduced MVP generated following PDT. There was, however, no difference when they were combined. The data depicted are mean SE fold change in MVP count (average of n=5). Groups were compared using one-way ANOVA and Tukey's post-hoc test. Differences in samples were considered significant if P is less than 0.05. P<0.05 (\*), P<0.01(\*\*), P<0.001(\*\*\*) and ns denotes not significant. . . . . 28
- 4.8 Imipramine inhibits production of MVPs by PDT in vitro. HaCaT cells (a) NTERTs (b) and Fibroblasts (c) were treated with 50M imipramine, a known aSMase inhibitor, immediately after PDT. Other groups were treated with 100nm CPAF, 500nm PMA or 0.1%EtOH (Veh). Imipramine was able to inhibit production of MVPs by PDT significantly across these 3 cell lines. The data depicted are mean SE fold change in MVP count (average of n=8). Groups were compared using one-way ANOVA and Tukey's post-hoc test. Differences in samples were considered significant if P is less than 0.05. P<0.05 (\*), P<0.01(\*\*), P<0.001(\*\*\*) and ns denotes not significant . . . . . 30
- 4.9 Imipramine inhibits production of MVPs by PDT in human skin explants ex vivo. Abdominoplasty skin explant was treated with 90% DMSO in 10% EtOH vehicle, 1mM 5 Aminolevulinic acid (5-ALA), 500ng PMA in 100L DMSO, 250ng CPAF in 100L DMSO, Blue light alone, PDT and had 50mM imipramine applied immediately after blue light exposure. Punch biopsies were taken after 4hrs incubation at 37C. Other groups were treated as earlier described. Imipramine was able to inhibit production of MVPs by PDT significantly in human skin. The data depicted are mean SE fold change in MVP count (average of n=5). Groups were compared using one-way ANOVA and Tukey's post-hoc test. Differences in samples were considered significant if P is less than 0.05. P<0.05 (\*), P<0.01(\*\*) . . . . . 31
- 4.10 Imipramine inhibits production of MVPs by PDT in vivo. C57BL6 mice had their backs shaved and received PDT. Imipramine was applied immediately after blue light exposure. Punch biopsies and blood samples were taken after 4hrs incubation at 37C. Other groups were treated as earlier described. Imipramine was able to inhibit production of MVPs by PDT both in the skin and plasma. The data depicted are mean SE fold change in MVP count (average of n=5). Groups were compared using one-way ANOVA and Tukey's post-hoc test. Differences in samples were considered significant if P is less than 0.05. P<0.05 (\*), P<0.01(\*\*), P<0.001(\*\*\*) 32

- 4.11 Role of acid sphingomyelinase in PDT-induced MVP release. C57BL6 and Smpd1 KO mice had their backs shaved and had PDT done as previously. There was no significant MVP generation following PDT in the Smpd1 KO mice unlike the C57BL6 strains. This further strongly suggests the major role aSMase plays in the generation of PDT-induced MVP. The data depicted are mean SD fold change in MVP count (n=4mice from a single experiment). Groups were compared using student's paired t-test. Differences in samples were considered significant if P is less than 0.05. P<0.05 (\*), P<0.01(\*\*), P<0.001(\*\*\*) and ns denotes not significant . . . . . 32
- 4.12 Role of PAFR in PDT-induced MVP generation using pafr +/- KB cells. PAFR-bearing KBP cells and PAFR negative KBM cells were treated with 100nm CPAF, 500nm PMA, PDT at 20J/cm<sup>2</sup> and incubated for 4hours before being processed for MVP isolation. PDT generated significant amount of MVP compared to the no treatment groups, suggesting a PAFR-independent process. The data depicted are mean SE fold change in MVP count (n=10). Groups were compared using one-way ANOVA and Tukey's post-hoc test. Differences in samples were considered significant if P is less than 0.05. P<0.05 (\*), P<0.0001(\*\*\*\*) and ns denotes not significant . . . . . 34
- 4.13 Role of PAFR in PDT-induced MVP. C57BL6 and pafr KO mice had their backs shaved and had PDT done as previously, with 250ng of CPAF. MVP generation in both groups of mice was significantly increased when compared to the sham groups. However, PDT did not generate a significant increase in MVP on the pafr KO skin. This could suggest a partial involvement of the PAFR in PDT-induced MVP generation. The data depicted are mean SD fold change in MVP count (n=6 mice). Groups were compared using one-way ANOVA and Tukey's post-hoc test. Differences in samples were considered significant if P is less than 0.05. P<0.05 (\*), P<0.01(\*\*) and ns denotes not significant. . . . . 34
- 6.1 PAFR expression in KB cells and human fibroblasts. Total RNA was extracted from KB cells and Fibroblast by TRIzol and extracted RNA was quantified with Nanodrop One (thermo fisher). High-Capacity cDNA Reverse Transcription kit was used to transcribed RNA samples to cDNA for the analysis of the PAF-R mRNA expression using a SYBR green-based, quantitative fluorescent PCR method. The fluorescence was detected using a StepOne Real-Time PCR machine (Applied Biosystems, Foster City, CA, USA). Primers were specific for PAF-R, GAPDH (as an endogenous control) and PAF-R expression in these cell lines were compared with stably PAF-R-expressing cell line-KBP and PAF-R-deficient cell line-KBM as positive and negative controls. The quantification of each PCR product was normalized to GAPDH using the 2- $\Delta\Delta$ Ct method. . . . . 39

- 6.2 Dose response curve of PDT-induced MVP release in fibroblasts. Primary cultures of human fibroblasts either received No treatment (NT), 500ng PMA in 3ml HBSS+BSA, 100ng CPAF in 3ml HBSS+BSA, 2.5J PDT (208secs), 5J PDT (416secs), 10J PDT (832secs) or 20J PDT (1663secs). PMA and CPAF being positive and negative controls respectively. A progressive increase in MVP count was obtained as PDT dose increased, reaching a peak at 20J. The data depicted are mean + SE fold change in MVP count (average of n=2). Groups were compared using one-way ANOVA and Tukey's post-hoc test. Differences in samples were considered significant if the P value was less than 0.05. P<0.05 (\*), P<0.001(\*\*\*) and P<0.0001(\*\*\*\*). . . . . 40
- 6.3 Relative survival rate of HaCaT cells following Antioxidant treatment. HaCaT cells had different concentrations of the antioxidants Vitamin C (VitC) and N-acetylcysteine (NAC) dissolved in fresh complete media and were incubated for 1hour at 37C. Plates subsequently had Trypan blue staining as described earlier and cell count was done with the Countess® machine. Cell count is taken as a percentage of the no treatment (NT) count. Higher doses of VitC and NAC significantly decreased cell count, appearing toxic. The data depicted are mean SE fold change in MVP count (average of n=3). Groups were compared using one-way ANOVA and Tukey's post-hoc test. Differences in samples were considered significant if P value is less than 0.05. P<0.001(\*\*\*) and P<0.0001(\*\*\*\*). . . . . 41
- 6.4 Effect of antioxidants on PMA- and CPAF-treated HaCaT cells. HaCaT cells were pre-treated with 0.5mM VitC and NAC for 1hour at 37C. They subsequently had 500ng PMA and 100ng CPAF both in 3ml HBSS+BSA treatments and were incubated for 4hours at 37C. Supernatants were harvested and processed for MVP isolation. Antioxidants reduced significantly the MVP generated by CPAF unlike PMA treated cells. The data depicted are mean SE fold change in MVP count (average of n=4). Groups were compared using one-way ANOVA and Tukey's post-hoc test. Differences in samples were considered significant if P value is less than 0.05. P<0.05(\*), P<0.01(\*\*), P<0.001(\*\*\*), P<0.0001(\*\*\*\*) and ns denotes not significant. . . . . 42
- 6.5 Imipramine inhibits production of MVPs by PDT in KB cells. KBP (a) and KBM (b) cells were treated with 50M imipramine, a known aSMase inhibitor, immediately after PDT. Other groups were treated with 100nm CPAF, 500nm PMA or 0.1%EtOH (Veh). Imipramine was able to inhibit production of MVPs by PDT significantly in these 2 cell lines. The data depicted are mean SE fold change in MVP count (average of n=8). Groups were compared using one-way ANOVA and Tukey's post-hoc test. Differences in samples were considered significant if P is less than 0.05. P<0.05 (\*), P<0.01(\*\*), P<0.001(\*\*\*), P<0.0001(\*\*\*\*). . . . . 43

6.6	Antioxidants inhibits production of MVPs by PDT in KB cells. KBP (a) and KBM (b) cells had 5-ALA incubation in the dark for 4hrs and were then treated with the antioxidants, 0.5mM Vitamin C (VitC) and 0.5mM N-acetylcysteine (NAC) for 1hour. Cells were subsequently exposed to blue light and supernatant were harvested 4hrs later. Other groups were treated as earlier described. Both antioxidants significantly reduced MVP generated following PDT. There was, however, no difference when they were combined. The data depicted are mean SE fold change in MVP count (average of n=5). Groups were compared using one-way ANOVA and Tukey's post-hoc test. Differences in samples were considered significant if P is less than 0.05. P<0.05 (*), P<0.01(**), P<0.001(***) , P<0.0001(****) and ns denotes not significant. . . . .	43
6.7	Groups of mice undergoing blue light treatment. . . . .	44
6.8	Skin preparation for PDT treatment. . . . .	45

# Acknowledgment

I would like to appreciate my mentor Dr. Jeffrey B. Travers, whose quintessential and magnanimous guidance made this project a success. My gratitude also goes to my committee members Dr. Ravi Sahu and Dr. Ji Chen Bihl. I appreciate your corrections and words of encouragement. I will forever appreciate the support of our lab manager, Christine Rapp, whose step-by-step tutelage and support contributed significantly to this project. Sincere appreciation to Langni Liu, Dr. Michael Kemp, Dr. Tetyana Zhelay, Avinash Mahajan, Pariksha Thapa, Ramzi Elased, Christina Borchers, Dr. Chen's Lab, and the entire Pharmacology and Toxicology Department. I appreciate greatly the support of my family and friends.

Studies funded by NIH R01 HL062996 and VA Basic Merit Grant BX000853.

Dedicated to

I dedicate this project to my dear family - my siblings and late parents, who never stopped believing in me and gave their all to give me a good head-start to life.

# Introduction

## 1.1 Statement of problem

Topical Photodynamic therapy (PDT), although a local therapy has been shown to exert systemic effects through poorly understood mechanisms. Microvesicle Particles (MVP) released from cells have been reported to play vital roles in cellular communication. This has stimulated research into their functions and properties, as biomarkers, therapeutic targets, and mediators of disease conditions. We believe that MVPs are involved in the systemic effects exerted by PDT. Thus, finding that PDT generates MVP in skin is an important question.

## 1.2 Significance

If MVPs are involved in the systemic effects of PDT, understanding the role and mechanism of release, can help to modify and widen the applications of PDT.

## 1.3 Statement of Purpose

The purpose of this project is to study the generation of MVP following PDT. Thus, we intend to answer a handful of questions pertaining to the release of MVP following PDT

such as: Does PDT generate MVP? Can this release be blocked? What mechanisms are involved in this release?

## 1.4 Hypothesis

Our central hypothesis is that PDT generates systemic effects via the generation of MVPs. Along with this, we expect that this release will be successfully blocked by antioxidants and the acid sphingomyelinase inhibitor, Imipramine.

## 1.5 Research objectives

- To demonstrate the release of MVP following PDT
- To define the mechanisms of MVP release following PDT
- To demonstrate effective blockage of MVP release following PDT

## 1.6 Definitions

**Abdominoplasty:** A surgical procedure that involves the removal of extra skin and or adipose tissue from the abdomen.

**Acid Sphingomyelinase (aSMase):** An enzyme that catalyzes the breakdown of sphingomyelin into ceramide. aSMase is a member of the sphingomyelinase family unique in its optimal acidic pH of 4.5—5.0.

**Carbamoyl-PAF (CPAF):** 1-alkyl-2-acetyl-glycerophosphocholine, a non-hydrolyzable PAF analog.

**Dimethyl sulfoxide (DMSO):** A universal solvent with the chemical formula  $(\text{CH}_3)_2\text{SO}$ . When compounds are dissolved in this solvent, they can easily penetrate the skin or cell



membrane.

**Dulbecco's Modified Eagle Medium (DMEM):** A common cell culture media to grow mammalian cells.

**HaCaT (Heat and Calcium Transformed cells):** These cells, which are aneuploid, were originally spontaneously transformed keratinocytes from histologically normal skin but have become immortalized.

**Hanks' Balanced Salt Solution (HBSS):** A buffer solution that contains calcium and magnesium to support cell adhesion.

**KBM:** A cell line (KB) derived from human, nasopharyngeal carcinoma. These cells underwent retroviral-mediated transduction with a blank vector, and do not express the PAF-R.

**KBP:** A cell line (KB) derived from human, nasopharyngeal carcinoma. These cells underwent retroviral-mediated transduction with a blank vector with a functional PAF-R.

**Knockout (KO):** When referring to a mouse, a knockout mouse has been genetically altered to not express a protein of interest.

**Microvesicle particle (MVP):** Also known as microvesicles and microparticles, are small membrane-bound particles with a diameter between 100-1000 nm that can be shed from the surface of virtually all eukaryotic cells in an active energy-dependent process.

**NTERT:** Immortalized human keratinocyte cell line expressing TERT made by transducing primary human keratinocytes with human telomerase reverse transcriptase (hTERT).

**PAF- receptor (PAF-R):** Platelet-Activating Factor Receptor, a G-protein coupled receptor which binds to PAF.

**Photodynamic therapy (PDT):** an adaptation of phototherapy, which involves the use of a photosensitizing drug with light of appropriate wavelength to cause cell damage.

**Phosphate Buffered Saline (PBS):** A buffer solution used for a variety of cell culture applications, such as washing cells before passaging, transporting cells or tissue, diluting cells for counting, and preparing reagents.

**Photosensitizer (PS):** An agent that can produce a chemical change in another agent when irradiated, through a photochemical process.

**Platelet-Activating Factor (PAF):** Acetyl-glycerol-ether-phosphorylcholine, potent phospholipid activator and mediator of many leukocyte functions, platelet aggregation and degranulation, inflammation, and anaphylaxis. PAF is produced by a variety of cells, but especially those involved in host defense, such as platelets, endothelial cells, neutrophils, monocytes, and macrophages.

**Reactive Oxygen Species (ROS):** Chemically reactive molecules that contain oxygen, examples include superoxide, singlet oxygen, peroxides, and hydroxyl radical.

## 1.7 Assumptions

In this project, it is assumed that cells will react similarly to the various treatments as a cell in a living organism. It is also assumed that there were no outside influences on the cell's reactions. For skin samples, it is assumed that all skin samples from the different patients will react similarly to the treatments. It is assumed that age, gender, and ethnicity will not affect MVP release from the various treatments. With the mouse model, it was assumed that the mice would react severally to the various treatments. It was also assumed that age and gender did not affect the MVP response to the treatments.

# Literature Review

## 2.1 Photodynamic therapy

Photodynamic therapy (PDT) is a therapy that presents an effective way to get rid of unhealthy (i.e precancerous and cancerous) cells. It involves an interplay between light acting on a photosensitive (PS) drug/chemical to generate reactive oxygen species (ROS) causing cytotoxicity [88][65][79][118][31]. Targeted cytotoxic cellular destruction occurs when tumor cells absorb and retain photosensitizers and are subsequently illuminated with visible light [5]. PDT is effective in treating superficial skin cancers. It is effective in the management of actinic keratoses, superficial basal cell carcinomas, as well as low-risk nodular basal cell carcinomas outside the head and neck region [100][84][105]. Other conditions that have been noted to respond to PDT include psoriasis, warts, mycosis fungoides, extramammary Paget's disease, and off-label uses for facial rejuvenation, and mild-to-moderate acne have been documented [100][102]. ROS are produced when photosensitizers accumulate, either actively or passively in tumor cells and are exposed to light of appropriate wavelength. Accumulation of the photosensitizer in the tumor cells greatly determines the efficacy of the generation of ROS for tumor destruction and thus, overall efficiency of PDT treatment[81]. PDT is a local therapy that is not expected to exert long-term systemic side effect [110]. With proper application, PDT carries little risk of long-term side effects. However, accumulation of the photosensitizer in surrounding healthy cells could cause some side effects. Unlike radiation, it can be repeated many times, it is less invasive than

surgery and has the advantage of being targeted more precisely, compared to chemotherapy [74]. With the observation of systemic immunosuppression following PDT [48][38][73], it became imperative to investigate the possible mechanisms through which this local therapy can exert systemic effects. This project is one of such attempts, in which we examined the involvement of certain cellular communication agents in the systemic response to PDT. We believe that these agents are released along with the photochemical products mediating local PDT effects.

### 2.1.1 Photochemical reactions in PDT

When a PS drug is exposed to light at appropriate wavelength, the PS drug gets excited from the ground state to an excited triplet state [88][73]. This excited PS molecule then transfers energy to Oxygen molecules converting them from the ground triplet state ( $^3O_2$ ) to the excited singlet state ( $^1O_2$ ) [57][114][33]. This transfer of quanta energy from the excited triplet PS molecule has been shown to occur in two pathways designated as Type I and Type II photochemical reactions Fig.2.1. Type I photochemical reaction involves the formation of free radicals which can react with molecular oxygen to generate ROS. Superoxide anions thus formed, mediate oxidative stress within the cell [2] and can also form hydrogen peroxide  $H_2O_2$  which easily pass through biological membranes to cause damage. Through the Haber Weiss reaction Fig.2.1,  $H_2O_2$  can react with superoxide anions at high concentrations to produce highly reactive hydroxyl radical, which can mediate further cellular damage.  $H_2O_2$  can also generate hydroxyl radicals by reacting with metals such as iron or copper, via the Fenton reaction as shown in Fig.2.1. Type II photochemical reaction involve the direct transfer of energy to molecular oxygen to generate high yield of highly reactive excited singlet oxygen molecules [28]. Of these two fundamental PDT reactions, the type II occurs predominantly with most PD drugs in circulation, although both reactions occur in parallel [114][33][103]. We do believe that these photochemical reactions also release certain agents that mediate intercellular communication and could be

strongly involved in the systemic effects exerted by PDT.

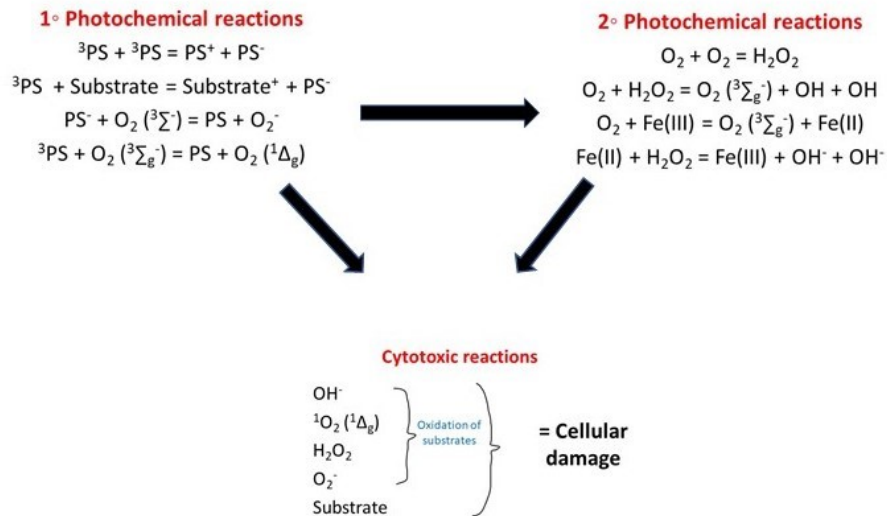


Figure 2.1: Overview of photochemical reactions during PDT. Several types of primary and secondary photochemical reactions cause production of reactive oxygen species and dose-dependent cellular damage.  $\text{H}_2\text{O}_2$ , hydrogen peroxide;  $\text{O}_2 ({}^1\Delta_g)$ , singlet oxygen (excited state);  $\text{O}_2 ({}^3\Sigma_g^-)$ , triplet oxygen (ground state);  $\text{O}_2^-$ , superoxide anion;  $\text{OH}^-$ , hydroxyl radical; SOD, superoxide dismutase;  $X^{-/+}$ , anion/cation species;  $X^{\cdot}$ , radical species. Adapted from ref ([88])

## 2.1.2 Photosensitizers

A photosensitizer (PS) is a molecule or drug that can be absorbed by cells and capable of generating photoproducts when exposed to light at appropriate wavelength [80]. These photoproducts through series of reaction described above react with oxygen (see Fig.2.1). Most PS employed in PDT are capable of generating high quantum yields of singlet oxygen molecules required for tissue damage [6]. Protoporphyrin IX (PPIX) is the photosensitive molecule believed to be the bedrock of PDT reactions [116][59][21] and this has been formulated for synthetic production in different forms. Studies investigating the accumulation of porphyrin at tumor sites shows its dependence on disturbances in the enzymatic framework of the heme pathway [17][44]. Notably, an inhibition of the enzyme ferrochelatase

leads to defective heme production and thus, a negative feedback which would favor the accumulation of PPIX within the tumor cells; see Fig.2.2 [19]. Apart from PPIX, other tumor-specific photosensitizers that have been identified include coproporphyrin and uroporphyrin [40][12][39]. Apart from use in PDT, through the use of a photodynamic fluorescence diagnosis technology, a photosensitizer can be adapted to diagnose tumors and possibly know its extent [50]. This is achievable as most photosensitizers are capable of fluorescence [7][23]. The ideal photosensitizer is one that is able to achieve preferential accumulation within tumor sites [32]. ALA has been shown to generate exponentially high levels of porphyrin in tumor cells as compared to normal skin cells, thus making it an admirable photosensitizer for PDT purposes [39][46]. Apart from selectivity, other desirable properties of an ideal PS include amphiphilicity (ability to be transported in blood without precipitating and gaining effective cell membrane penetration) [89], must not be toxic or have mutagenic effects[10], safe with minimal side effects and rapid clearing from the body [115].

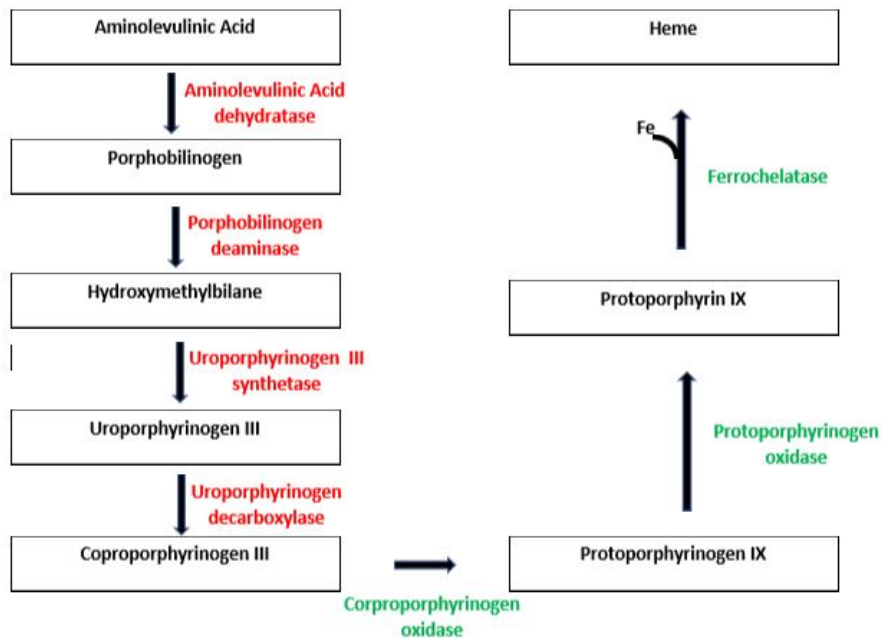


Figure 2.2: Biosynthesis of heme in mammals. Mitochondrial enzymes are in green while cytosolic enzymes are in red. Adapted from ref [8]

### 2.1.3 Applications of PDT

PDT has found wide application in oncology following the study of hematoporphyrin derivatives (HpD) and its clinical uses in the 70s [109]. It has been well-argued that the unique redox regulatory mechanisms of cancer cells can be modulated leading to effective therapeutic means to destroy cancer cells [108][104]. By generating free radicals and reactive oxygen species within cells, this redox environment so created has been shown to be dangerous for normal cell sustainability due to the increased oxidative stress, both on the membrane and the cytosolic organelles, as well as the nucleus [95][47][15][45]. PDT is more efficient for non-small cell lung tumors that are still within the lungs, and is used as an adjunct to Chemotherapy or radiation, for metastatic tumors [98][77]. With selective delivery of PDT to tumor sites, PDT poses as a minimally invasive alternative to other conventional cancer therapies like surgery, and limits damage to neighboring healthy tissues [109][52]. While PDT has been largely used in oncology since its discovery, within the last decade, it has gained significant application outside oncology [88]. PDT has shown significant favorable applications in dermatology. Apart from its use in certain skin cancers, PDT presents an effective therapeutic option in the management of actinic keratosis, acne vulgaris [93][29], psoriasis, warts, impetigo. In the last decade, PDT has also been explored widely for its antimicrobial properties [26][43][75][56][34].

## 2.2 Microvesicle Particles

Microvesicle particles (MVP), also called microparticles, microvesicles, ectosomes, belong to a group of cell membrane-derived particles, called extracellular vesicles (EVs) [90]. This group comprises exosomes, MVPs and apoptotic bodies (Fig.2.3). Although it is currently difficult to clearly delineate these particles, mode of formation and size are two promising factors that can be used to classify them [90]. Recent guidelines in the classification of EVs adopted the use of Large extracellular vesicles for MVPs and Small extracellular vesicles

for exosomes [107]. EVs were previously regarded as cell debris but have gained a progressive attention as potential biomarkers or mediators of several metabolic processes in the last decade [72][66]. Together with cell-to-cell contacts and cytokines, EVs have been found to play a role in cellular communication [20]. MVPs are spherical, membrane-bound particles with a diameter of 150-1000nm, that bud directly off cell membrane surfaces [3]. They are secreted by all eukaryotic cell types due to various stimulus including serum withdrawal, shear stress and cytokine signaling [113]. Although not fully understood, few pathways have been identified to play a role in the release of MVPs. Amongst these, the P2X7R appears to be dominant [42][25]. Other identified pathways include mitogen-activated protein kinase (MAPK) pathway [67], small GTPases [82][11]. MVPs have been shown to contain various bioactive proteins, lipids, cytokines, nucleic acids, membrane receptors and adhesion molecules [90][72][9][22]. Apart from their roles in intercellular communication, MVPs have been explored as a biomarker, mediator of several conditions and potential targets for therapeutic interventions [71][117][111]. Following their involvement in the systemic effects induced by ultraviolet B (UVB) radiation [70][120], it is thus a possibility that MVPs can be possible mediators of PDT systemic effects.

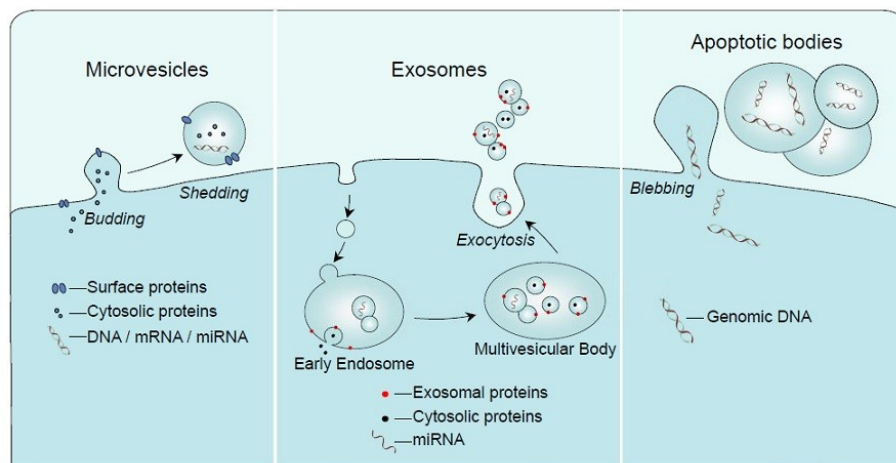


Figure 2.3: Schematic representation of the mechanisms of formation of microvesicles, exosomes and apoptotic bodies ([66])



## 2.3 Platelet Activating Factor Receptor

The platelet activating factor receptor (PAFR) is a G-protein coupled transmembrane receptor found on multiple types of classically immune cells as well as epithelial cells, through which the inflammatory phospholipid, platelet activator factor (1-alkyl-2-acetyl glycerol-phosphocholine; PAF) carries out its functions [120][91]. PAF mediates important systemic responses such as inflammation, allergic reactions, platelet aggregation. PAFR is activated by oxidized glycerophosphocholines (ox-GPC) produced when ROS acts on glycerophosphocholines (GPC). As such, pro-oxidative stressors such as cigarette smoke, jet fuel, UVB, chemotherapeutic agents can generate PAFR ligands needed to activate it [54][94][119]. It is thus possible that PDT, with its copious ROS yield, can generate PAFR ligands and ultimately, lead to its activation. A functional analog of PAF, carbamyl platelet activating factor (1-hexadecyl-2-N-methylcarbamyl-glycero-3-phosphocholine; CPAF) also has strong agonistic effects at the receptor, when bound [120][119][36]. Being non-metabolizable and relatively stable, this has been exploited for use in experimental set-ups, as done in this study and other studies involving the PAFR. A study involving our group, used *in vitro* and *in vivo* murine models to show the involvement of the PAFR in the systemic immunosuppression observed following topical PDT with 5-Aminolevulinic acid [38]. With the understanding that PAFR signaling releases MVPs following UVB irradiation [70][18], we believe that PDT, through generation of ROS and thus PAFR activation, can lead to MVP release.

# Materials and Methods

## 3.1 Introduction

This chapter discusses the experimental models, materials, procedures and analysis performed to generate the relevant data in line with the aim and objectives of this study. Basic models employed in this study include *in-vitro* cell lines, *ex vivo* human skin and *in vivo* murine model.

## 3.2 Cell Culture

Five cell lines were used in this study. Spindle-shaped Heat and Calcium transformed (Ha-CaT) cell line is derived from spontaneously immortalized human keratinocytes and like primary keratinocytes, they exhibit basal cell properties and are capable of responding to inducers of cell differentiation such as calcium and high cell density [97][83]. NTERT cells are immortalized primary keratinocytes expressing telomerase hTERT [30]. Normal Human Fibroblasts were derived primarily from human skin culture [60][37]. KB cells were primarily isolated from a patient with nasopharyngeal carcinoma, representing a human cell model without PAFR. The cells were later transduced with MSCV2.1 retrovirus containing PAF-R [KBP] and KBM cells with control MSCV2.1 retrovirus without PAF-R [120][86].

### **3.2.1 Cell Growth Media and Storage Condition**

HaCaT, Fibroblasts and KBP/ KBM cells were grown in DMEM media. Media consisted of a 500 mL bottle high glucose DMEM containing 100 U penicillin/ 0.1 mg/mL streptomycin (5mL), 2 mM glutamine (5 mL), and 50 mL 10% FBS FetalClone III. For NTERTs, EpiLife Growth media with human keratinocyte growth supplement (HKGS) 100x and 100 U penicillin/ 0.1 mg/mL streptomycin (5mL) was used. All the cells were kept at 37°C and 5% CO<sub>2</sub> in humidified incubator.

### **3.2.2 Cell Passage**

Media was removed from cells (KBs, HaCaT, Fibroblasts) and plates were washed 3 times with 10 mL of PBS 1X. 2 mL of 0.25% Trypsin-EDTA 1X (for HaCaT) and 0.05% Trypsin-EDTA 1X (For Fibroblasts and KB cells) was then added to each plate and placed in the incubator for 5-10 minutes. Then, 8 mL of media was added to each plate to bring it back to 10 mL and cells were tritured. 6 drops of the cells suspended in media was added to a new plate with 10 mL of fresh media. For NTERTs, plates were washed three times with 10 mL PBS 1X. Then, 2 mL of 0.05% Trypsin- EDTA 1X was added to each plate and placed in the incubator for 10 minutes. 6 mL of high glucose DMEM was then added to the plates and tritured. Cells which were to be treated, were counted before adding to the new plates to ensure that equal number of cells were added to each plate. For the sake of consistency of results, cells were counted and grown for equal number of days each time.

### **3.2.3 Changing Media**

To change media, the old media was removed from the culture plate and was washed 3x with PBS 1X. 10mL of fresh complete media was then added. Media change is done every 2-3 days between passaging.

### **3.2.4 Cell Counts**

Cells were first washed 3x with 10mL PBS 1x. 2-3mL 0.05% Trypsin was added and returned to the incubator for 5-7mins. As soon as the cells got detached, 8mL of fresh media was added to the plate. 10L of this suspended cell mixture was added to 10L Trypan blue stain. 10L of this resulting mixture is pipetted onto a slide and cell count was obtained on the Countess machine.

### **3.2.5 Bringing Up Cells from Liquid Nitrogen**

Vials containing cells were taken out from liquid nitrogen and allowed to thaw at room temperature. Cells were immediately added to a new culture plate containing 10mL of fresh media. 24hours later, cells were fed and then passed onto new plates.

### **3.2.6 Treatments**

3mL of Hank's Balanced Salt Solution and 10mg/mL Bovine serum albumin (HBSS+BSA) with desired concentration of treatment reagents were added to each plate. Sham culture plates received plain HBSS+BSA and were incubated for the desired length of time. Vehicle treated cells received 0.1% of Ethanol in HBSS+BSA. CPAF-treated cells received 3L of 100M CPAF added to 3mL of HBSS+BSA to obtain final concentration of 100nM. PMA treated cells received 3L of 500M PMA added to 3mL of HBSS+BSA calculated to final concentration of 500nM.

#### **PDT Treatment**

PDT was done by incubating cells with 1 mM of 5-Aminolevulinic acid (5-ALA) in complete media [62][63] in the dark for 4 hours as has been designed in this model [69][41]. 5-ALA-containing media was then discarded, cells were washed 3x with serum-free HBSS

and then embedded in 3mL of HBSS+BSA before subsequent exposure to blue LED light source 415nm at 20 J/cm (1663secs). For the dose response study, cells were exposed to different doses of blue light - 2.5J/cm<sup>2</sup> (207.875secs), 5J/cm<sup>2</sup> (415.75secs), 10J/cm<sup>2</sup> (831.5secs) and 20J/cm<sup>2</sup>. Supernatant was collected after 4hours of incubation.

### **3.2.7 Inhibitors**

Imipramine, an aSMase inhibitor (101) used in the experiments was added to the plate and incubated for 4 hours as with other treatments. 3L of 50mM imipramine with 3mL of HBSS+BSA was added to each plate to make final concentration of 50M. However, for PDT, Imipramine was added after the light exposure due to the sunscreen effect of imipramine. After 4hours incubation in the dark with 5-ALA, cells were washed 3x with serum-free HBSS. 0.5M Ascorbic acid (Vitamin C) and N-acetylcysteine (NAC) in fresh complete media was added to respective plates and incubated for 1hour. Plates were then washed again with serum-free HBSS and exposed to light at 20 J/cm (1663secs).

### **3.2.8 MVP Isolation**

After the determined incubation time, supernatant from the treated culture plates were transferred to 2mL centrifuge tubes and centrifuged immediately in microcentrifuge tubes at 2000xg for 20 minutes at 4°C. Then the supernatant was transferred to a new tube and centrifuged at 20,000xg for 70minutes. After the centrifugation, the supernatant was discarded, and tubes were allowed to air-dry. Pellet was re-suspended in 100L of filtered 1x PBS. The samples were analyzed with Nanosight NS300.

### **3.2.9 MVP Analysis**

The reading obtained from the Nanosight NS300 was multiplied by the dilution rate and then divided by the cell count. The total MVP count normalized with cell number were

multiplied by 100,00cells and calculated as fold change. The errors were calculated for each treatment groups, graphed on GraphPad Prism 8 and analyzed with one-way and two-way ANOVA to show significance with a 95% confidence interval.

### **3.3 MTT Assay for Cell Survival**

Medium was removed from plates after respective treatment. 1.25mL of 5mg/mL MTT solution was added to 23.75mL of Epilife medium (for 0.25mg/mL MTT final concentration MTT final concentration). 2mL of this MTT-containing medium was added to each plate and incubated for 45min at 37°C. Medium was then removed and replaced with 1mL of DMSO to solubilize MTT dye and was well mixed. 100L of the resulting solution was transferred to a 96-well plate, 3 wells per sample. Using the Microtek® plate reader, absorbance was read at 570nm. Cell survival was calculated by an average of 3 identical wells and normalized to the no treatment group.

### **3.4 Skin**

Abdominoplasty skin explants were obtained from Miami Valley Hospital, Dayton, Ohio. Patients were between the ages 36-65years.

#### **3.4.1 Treatment**

Skin was treated with either 90% DMSO in 10% EtOH vehicle, 250g CPAF made in vehicle, 500g PMA, 50mM Imipramine, 20 J/cm<sup>2</sup> PDT. PDT was performed by applying 100ng of 5-ALA on skin and incubating in the dark for 4hours with subsequent exposure to blue light at 20 J/cm<sup>2</sup> (1663secs). Imipramine was added immediately after PDT.

### **3.4.2 Punch Biopsies**

After treatment, the skin pieces were placed in a 37°C water bath in individual culture dishes. Then 6 mm punch biopsies were taken from the center of each piece of skin after 4 hours of incubation. Fatty tissues were removed, they were individually weighed and placed in separate Eppendorf® tubes. Tissues were covered in 500L of 5mg/mL collagenase dispase made in 1:1 H<sub>2</sub>O. The tissue was then cut up finely in the Eppendorf® tube and digested overnight in a shaker at 37°C.

### **3.4.3 MVP Extraction from Punch Biopsies**

After the overnight digestion of the tissue, the tubes were filled with an additional 1-1.5mL of PBS (1x) and centrifuged at 2000 x g for 20 minutes. Supernatant was moved to a new tube and centrifuged at 20,000 x g for 10 minutes. The supernatant was moved again to a new tube and centrifuge at 20,000 x g for 70 minutes. Supernatant was then discarded, and pellet was re-suspended in 100 L filtered PBS (1x). Samples were placed in -80C freezer until analysis.

## **3.5 Mice**

C57BL/6, Smpd1 KO and Pafr KO mice were recruited for use in this project. Mice were housed together, provided with water and food ad libitum in a 12 hours light and dark cycle room. The protocol for the experimental use of animals was approved by Wright State University, School of Medicine's Laboratory Animal Care and Use Committee (LACUC).

### **3.5.1 Treatment**

Mice were injected with ketamine/xylazine, shaved and treated with either 90% DMSO in 10% EtOH vehicle, 100g CPAF made in vehicle, 500g PMA made in vehicle, 50mM

Imipramine, 20 J/cm<sup>2</sup> PDT. PDT was performed by applying 20ng of 5-ALA on the shaved back of mice and kept in the dark for 4hours with subsequent exposure to blue light at 20 J/cm<sup>2</sup> (1663secs). Imipramine was added immediately after PDT.

### **3.5.2 Murine Punch Biopsies**

After 4hours of incubation, 5mm punch biopsies were taken from the treated skin on the back of each mice and each skin biopsies were individually weighed. The skin biopsies were placed in 2mL microcentrifuge tubes and 500L of 5mg/mL collagenase dispase made in 1:1 H<sub>2</sub>O was added to each tube. The tissue was finely chopped in the microcentrifuge tube and digested overnight in the shaker at 37C. After the overnight digestion, the tube was filled up with filtered PBS and then centrifuged at 2000xg for 20minutes. The supernatant is transferred to a clean microcentrifuge tube and centrifuged at 20,000xg for 10minutes. The supernatant is finally transferred to another clean microcentrifuge tube and centrifuged at 20,000xg for 70minutes. Supernatant was discarded and the pellet was re-suspended in 100mcl filtered PBS (1X). Samples were stored at 4°C until analysis.

### **3.5.3 Blood Sample Collection**

At the same time blood was collected from the mice, euthanized in CO<sub>2</sub> tank and cervically dislocated. The blood was drawn from the heart of a mice with 1ml of 30g BD syringe and collected in the microcentrifuge tubes. Blood plasma was isolated by centrifugation at 2000xg for 20min and the blood plasma (upper clear layer) was isolated and pipetted into a new tube carefully. The MVP was isolated after centrifugation at 2000xg for 20minutes and 20,000xg for 70 minutes.



### 3.6 Statistical Analysis

Mean and significance were determined, and graphs were made using GraphPad Prism 8. Data is expressed as mean standard error. Groups were compared using one-way ANOVA. Differences in sample were considered significant if the P values were less than 0.05. Notation within the figure include  $P < 0.05$  (\*),  $P < 0.01$  (\*\*),  $P < 0.001$  (\*\*\*) and  $P < 0.0001$  (\*\*\*\*).

# Results

## 4.1 Generations of MVPs following PDT

These studies were designed to study the pattern of generation of MVP generation following treatment with PDT.

### 4.1.1 PDT Dose Response in HaCaT Cells

To determine the optimal dose of PDT that can generate MVPs without exerting a toxic effect, different doses of blue light (2.5J, 5J, 10J, 20J) along with 5ALA were used on primary keratinocytes and incubated for 4 hours (Fig.4.1). HaCaT cells responded with progressive increase in MVP generation with the maximal response recorded with 20J, which is in line with previous studies using similar cells [38]. However, this increasing does response in MVP generation was accompanied by a corresponding decrease in cell survival rate, with the most lethal dose being 20J.

### 4.1.2 Time Response in MVP Generation following PDT

Conventional studies in PDT employ various time points depending on the end points desired, ranging from immediately post-treatment to as long as days. We sought to determine

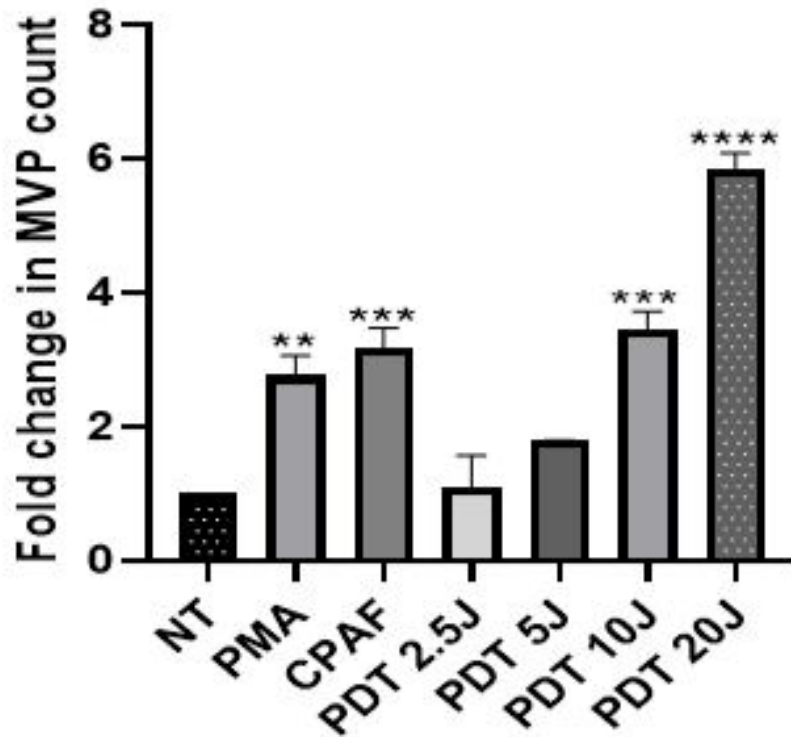


Figure 4.1: Dose response curve of PDT-induced MVP release in HaCaT cells. Cells either received No treatment (NT), 500ng PMA in 3mL HBSS+BSA, 100ng CPAF in 3mL HBSS+BSA, 2.5J PDT (208secs), 5J PDT (416secs), 10J PDT (832secs) or 20J PDT (1663secs). PMA and CPAF being positive controls generated 2-3 folds of MVP as compared to control. A progressive increase in MVP count was obtained as PDT dose increased, reaching a peak at 20J. The data depicted are mean  $\pm$  SE fold change in MVP count (average of n=3). Groups were compared using one-way ANOVA and Tukey's post-hoc test. Differences in samples were considered significant if the P value was less than 0.05.  $P < 0.05$  (\*),  $P < 0.01$ (\*\*),  $P < 0.001$ (\*\*\*) and  $P < 0.0001$ (\*\*\*\*).

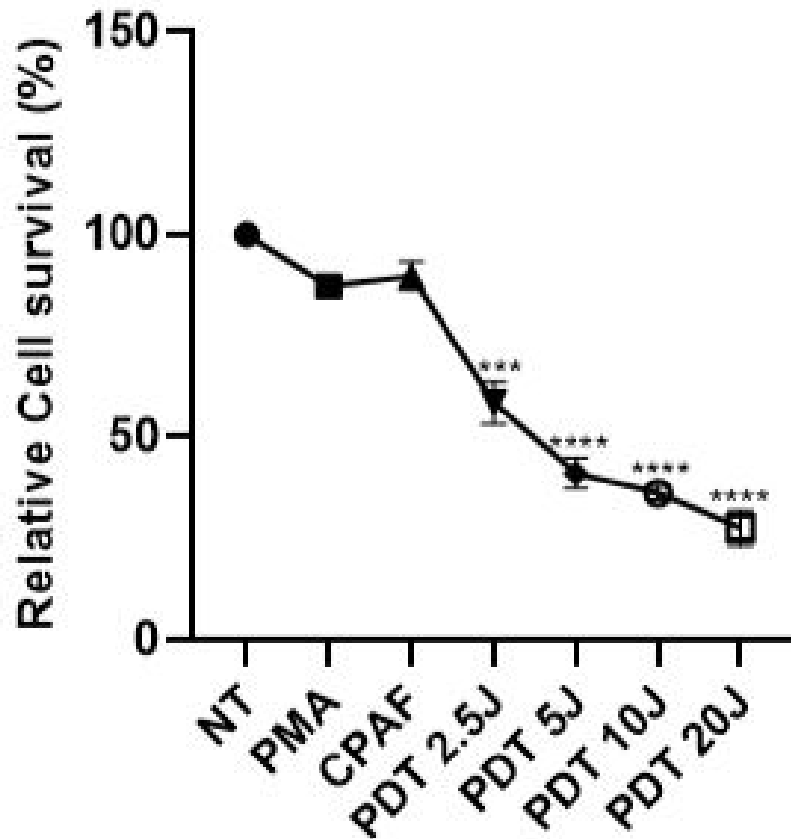


Figure 4.2: Relative survival rate of HaCaT cells following PDT treatment. After the different treatments in Fig. 4, cells were subjected to an MTT assay at 4hours post-treatment. A progressive decline in cell survival rate was seen as PDT dose increased, reaching the lowest at 20J suggesting the most lethal effect on cells. The data depicted are mean SE fold change in MVP count (average of n=3). Groups were compared using one-way ANOVA and Tukey's post-hoc test. Differences in samples were considered significant if P value is less than 0.05.  $P < 0.001$ (\*\*\*) and  $P < 0.0001$ (\*\*\*\*).

the optimal time point favorable for MVP generation. Primary keratinocytes were treated with PDT and lysates were harvested at different time points 0h, 2h, 4h, 8h and 24h. Maximum generation of MVP was observed 24hours post-PDT. However, this is comparable to the amount generated 4hrs post-PDT, with no significant difference.

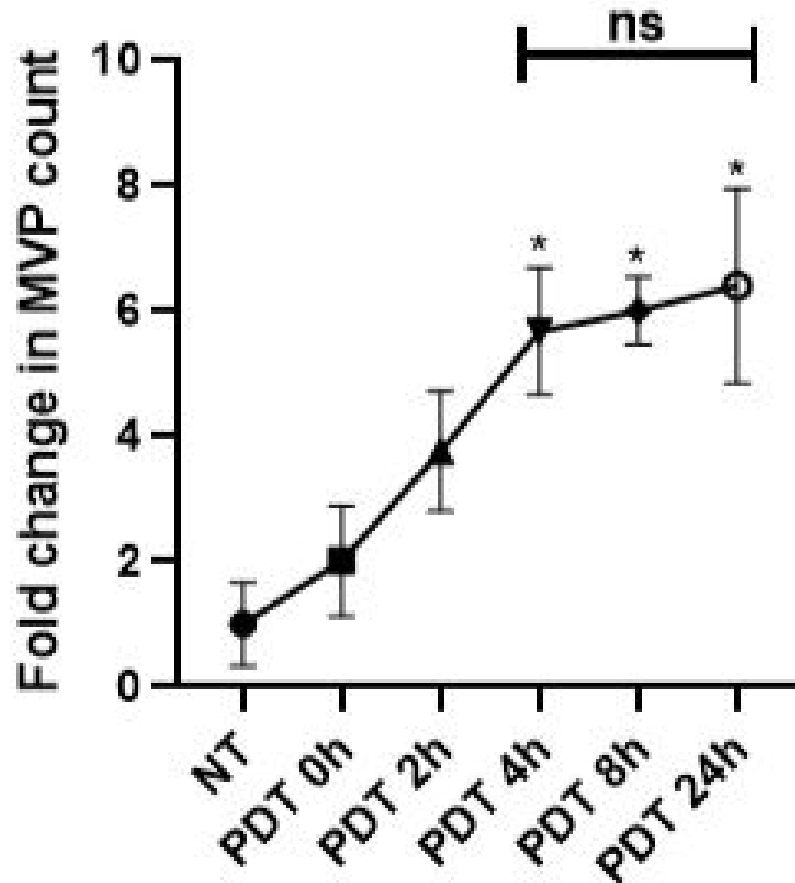


Figure 4.3: Time response of PDT-induced MVP production in HaCaT cells. After PDT treatment, supernatants were either harvested immediately (0h) or incubated for 2h, 4h, 8h or 24h before being collected for MVP isolation. A somewhat progressive increase occurred in MVP count as time progresses. There was, however, no significant difference between the count at 4h, 8h and 24h. The data depicted are mean SE fold change in MVP count (average of n=3). Groups were compared using one-way ANOVA and Tukey’s post-hoc test. Differences in samples were considered significant if P is less than 0.05. P<0.05 (\*), while ns denotes no significance.

### **4.1.3 Generation of PDT Across Different Cell Lines**

Primary keratinocytes (HaCaT), NTERTS, and normal human Fibroblasts were treated with 20J/cm<sup>2</sup> of PDT, with lysates collected after 4hrs based on time kinetic and dose data (Fig.4.1 and Fig.4.3). A significant increase in MVP generation was noted across these 3 cell lines.

### **4.1.4 Generation of MVP following PDT ex vivo**

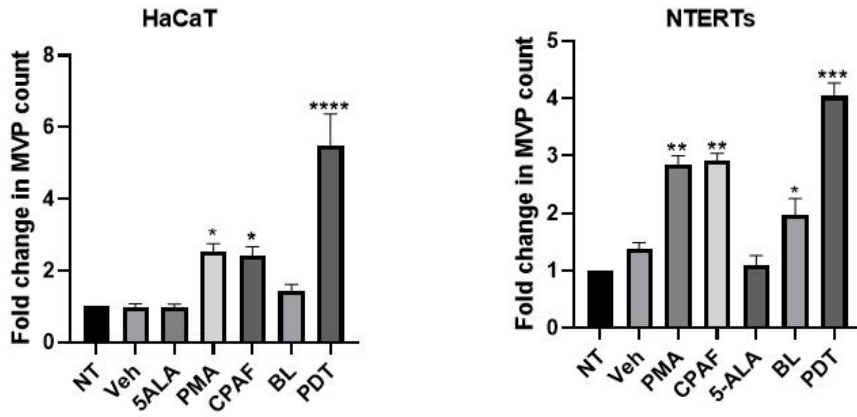
Human skin explants were treated with 20J/cm<sup>2</sup> of PDT and biopsies were taken after 4hrs of incubation at 37°C, with subsequent isolation and quantification of MVPs. PDT significantly generated increased levels of MVPs.

### **4.1.5 Generation of MVPs following PDT in vivo**

Anesthetized C57BL6 mice had their backs shaved followed by 20J/cm<sup>2</sup> of PDT treatment. Skin biopsy and Plasma samples were obtained after 4hrs. There was an increase in the amount of MVP generated in both skin and plasma samples.

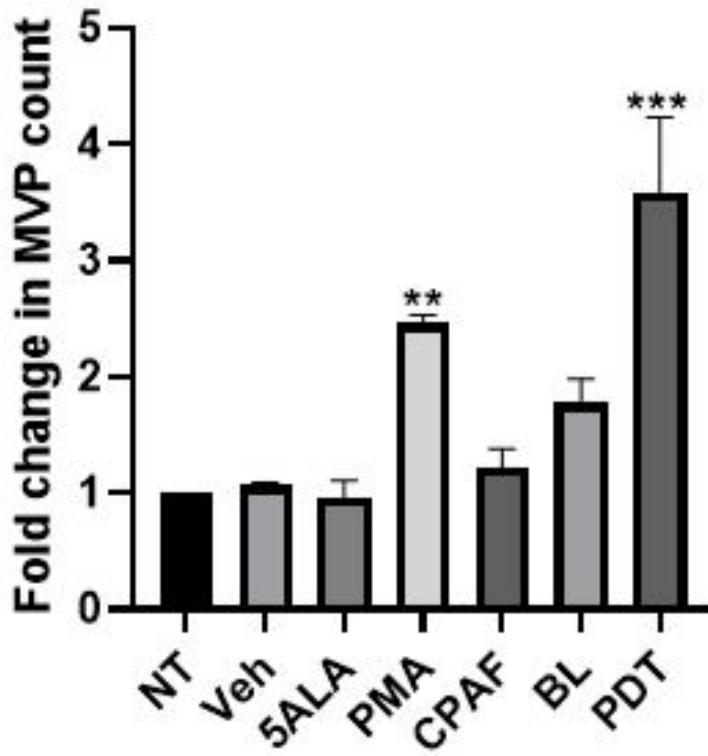
## **4.2 Role of Reactive Oxygen Species in the Generation of MVPs following PDT**

An established mechanism of PDT action is the generation of reactive oxygen species (ROS) [88][73][16][23]. These set of studies investigate the role of ROS in the generation of MVPs following PDT. Using the antioxidants Ascorbic acid (Vitamin C) and N-acetylcysteine (NAC), HaCaT cells were treated with these for 60mins, after incubation



(a)

### Fibroblasts



(b)

Figure 4.4: PDT generates MVPs across different cell types. HaCaT (a) NTERT (b) and Fibroblasts (c) were either treated with plain HbSS+BSA (NT), 0.1% EtOH (Veh), 1mM 5ALA, 500ng PMA, 100ng CPAF, Blue light alone (BL) or PDT and were incubated for 4hours. PDT generated significantly high amounts of MVPs across the 3 different cell lines. The data depicted are mean SE fold change in MVP count (average of n=8). Groups were compared using one-way ANOVA and Tukey's post-hoc test. Differences in samples were considered significant if P is less than 0.05. P<0.05 (\*), P<0.01(\*\*), P<0.001(\*\*\*) and P<0.0001(\*\*\*\*).

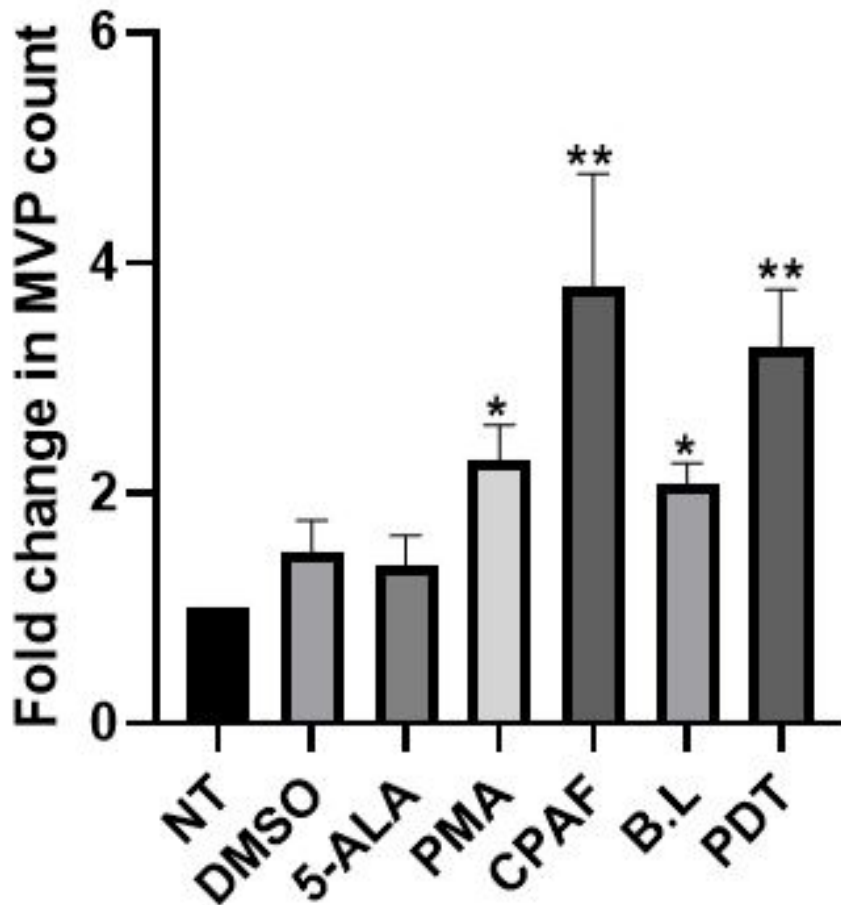


Figure 4.5: PDT generates MVPs ex vivo in human skin. Human skin explants were treated with nothing (NT), 90% DMSO in 10% EtOH, 100ng 5ALA, 500g PMA in 100L DMSO, 250g CPAF in 100L DMSO, Blue light alone (BL) or PDT and were incubated for 4hours at 37C after which biopsies were taken. PDT generated significant amount of MVP. The data depicted are mean + SE fold change in MVP count (average of n=5). Groups were compared using one-way ANOVA and Tukey's post-hoc test. Differences in samples were considered significant if P is less than 0.05. P<0.05 (\*) and P<0.01(\*\*).



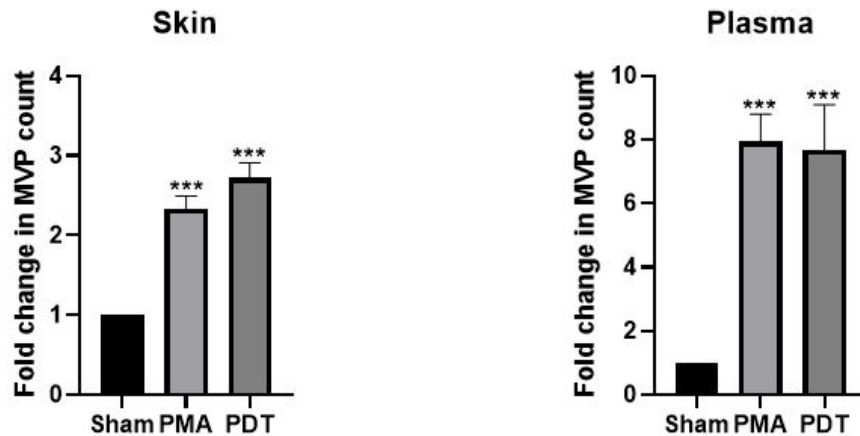


Figure 4.6: PDT generates MVPs in vivo in Mice skin. C57BL6 mice had their backs shaved and were treated with 90% DMSO (Sham), 500g PMA, or PDT. Biopsies and blood samples were taken after 4hours. PDT generated significant amount of MVP both in skin (a) and plasma (b). The data depicted are mean SE fold change in MVP count (data was from at least n=5mice). Groups were compared using one-way ANOVA and Tukey's post-hoc test. Differences in samples were considered significant if P is less than 0.05. P<0.001(\*\*\*).

with 5-ALA but prior to blue light exposure at 20J/cm<sup>2</sup>. Supernatants were collected following 4hrs of incubation at 37°C. As shown in Fig.4.6, both Vitamin C and NAC treatment significantly inhibited the MVP generated by PDT, alone and in combination.

### 4.3 Roles of aSMase in the Generation of MVP following PDT

To test the role of acid sphingomyelinase (aSMase) in the generation of MVP following PDT, a known inhibitor of the enzyme, imipramine [68][24] was used on cells, skin explant and mice skin. Because imipramine can absorb UV, it was given after the blue light.

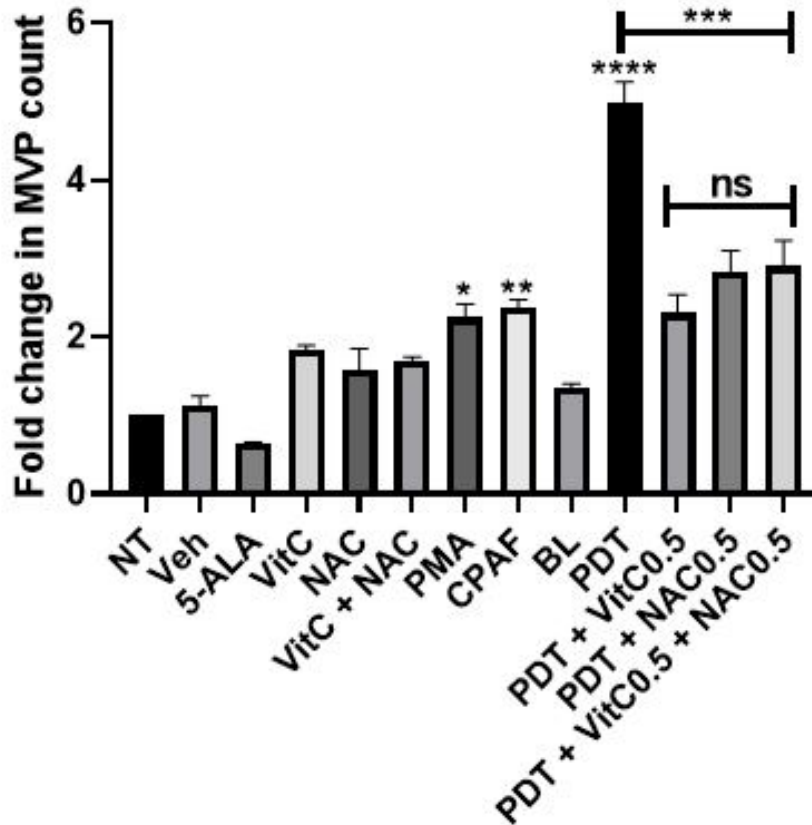


Figure 4.7: Antioxidants inhibit production of MVPs by PDT in vitro. HaCaT cells had 5-ALA incubation in the dark for 4hrs and were then treated with the antioxidants, 0.5mM Vitamin C (VitC) and 0.5mM N-acetylcysteine (NAC) for 1hour. Cells were subsequently exposed to blue light and supernatant were harvested 4hrs later. Other groups were treated as earlier described. Both antioxidants significantly reduced MVP generated following PDT. There was, however, no difference when they were combined. The data depicted are mean SE fold change in MVP count (average of n=5). Groups were compared using one-way ANOVA and Tukey's post-hoc test. Differences in samples were considered significant if P is less than 0.05. P<0.05 (\*), P<0.01(\*\*), P<0.001(\*\*\*) and P<0.0001(\*\*\*\*) and ns denotes not significant.

### **4.3.1 Roles of aSMase in the Generation of MVP following PDT in cells**

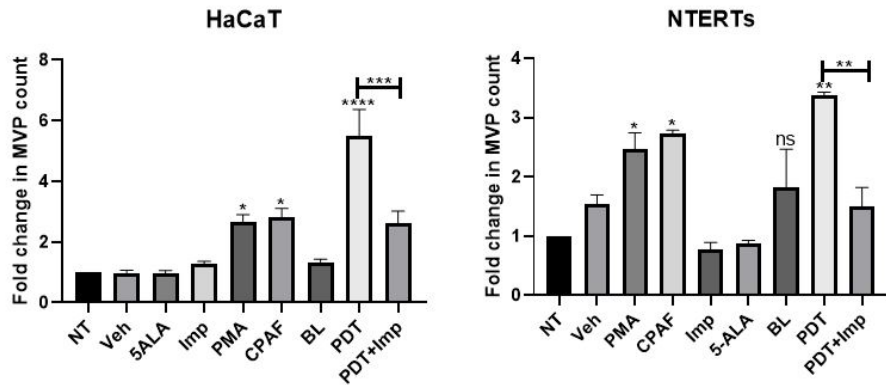
Different cell lines – HaCaT, NTERTS and primary cultures of human fibroblasts were treated with PDT, imipramine was added immediately after exposure to blue light and supernatants were harvested after 4hrs. As shown in Fig.4.7, imipramine was able to significantly reduce the production of MVPs following PDT in these cell lines. On some experiments, cells were treated with CPAF or the PKC agonist, PMA.

### **4.3.2 Role of aSMase in PDT-generated MVP in Skin**

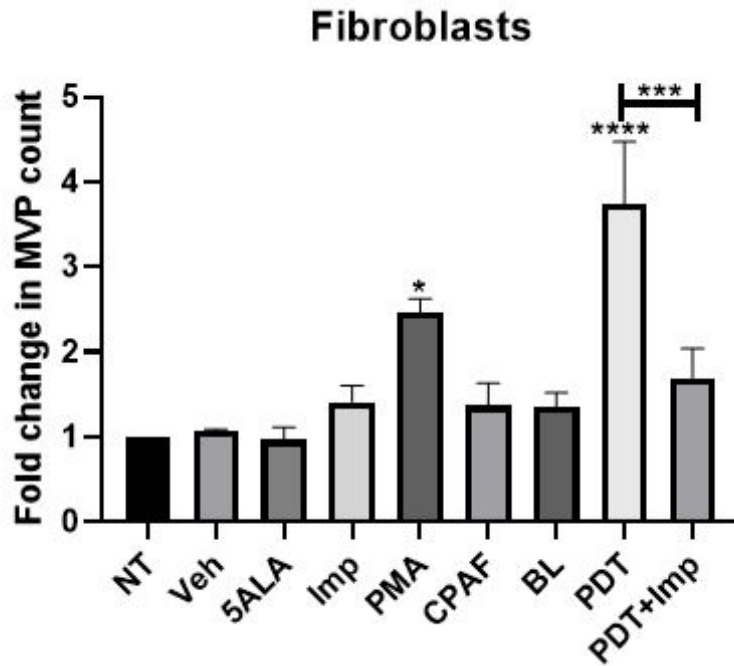
The next studies were designed to test if the aSMase inhibitor, imipramine, can block MVP generation in human skin explants in response to experimental PDT. Following the previous PDT protocol, skin explants were treated with imipramine immediately after blue light exposure and punch biopsies were taken 4hrs later. Imipramine was able to reduce significantly, the level of MVP generated by PDT.

### **4.3.3 Role of aSMase in PDT-generated MVP in mice**

The next studies tested the role of aSMase *in vivo* using knock-out mice. C57BL6 and aSMase-deficient (Smpd1 *-/-*) mice were recruited to test the role of aSMase in the generation of MVP following PDT. The anesthetized mice had their backs shaved with the topical application of 5-ALA and subsequent exposure to blue light. Imipramine was applied topically immediately after light exposure. Skin biopsies and plasma samples were taken after 4hrs. As shown in Fig.4.8, imipramine treatment resulted in a reduction in the production of MVPs by PDT.



(a)



(b)

Figure 4.8: Imipramine inhibits production of MVPs by PDT in vitro. HaCaT cells (a) NTERTs (b) and Fibroblasts (c) were treated with 50M imipramine, a known aSMase inhibitor, immediately after PDT. Other groups were treated with 100nm CPAF, 500nm PMA or 0.1%EtOH (Veh). Imipramine was able to inhibit production of MVPs by PDT significantly across these 3 cell lines. The data depicted are mean SE fold change in MVP count (average of n=8). Groups were compared using one-way ANOVA and Tukey's post-hoc test. Differences in samples were considered significant if P is less than 0.05. P<0.05 (\*), P<0.01(\*\*), P<0.001(\*\*\*) and ns denotes not significant

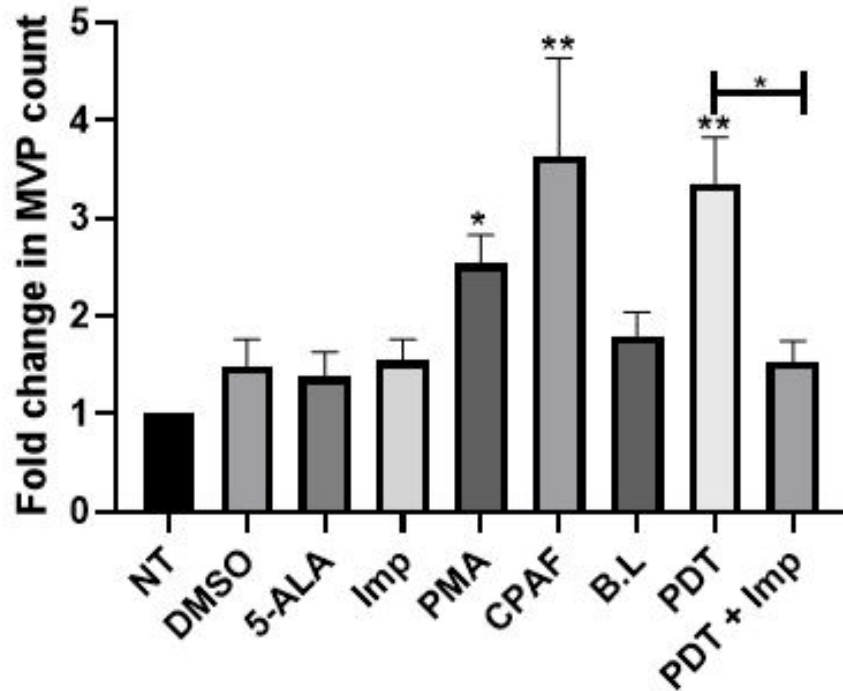


Figure 4.9: Imipramine inhibits production of MVPs by PDT in human skin explants ex vivo. Abdominoplasty skin explant was treated with 90% DMSO in 10% EtOH vehicle, 1mM 5 Aminolevulinic acid (5-ALA), 500ng PMA in 100L DMSO, 250ng CPAF in 100L DMSO, Blue light alone, PDT and had 50mM imipramine applied immediately after blue light exposure. Punch biopsies were taken after 4hrs incubation at 37C. Other groups were treated as earlier described. Imipramine was able to inhibit production of MVPs by PDT significantly in human skin. The data depicted are mean SE fold change in MVP count (average of n=5). Groups were compared using one-way ANOVA and Tukey's post-hoc test. Differences in samples were considered significant if P is less than 0.05. P<0.05 (\*), P<0.01(\*\*)

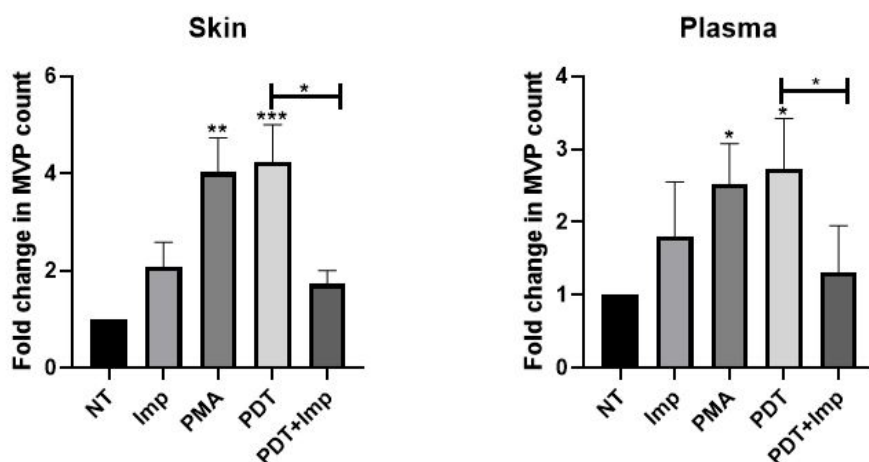


Figure 4.10: Imipramine inhibits production of MVPs by PDT in vivo. C57BL6 mice had their backs shaved and received PDT. Imipramine was applied immediately after blue light exposure. Punch biopsies and blood samples were taken after 4hrs incubation at 37C. Other groups were treated as earlier described. Imipramine was able to inhibit production of MVPs by PDT both in the skin and plasma. The data depicted are mean SE fold change in MVP count (average of n=5). Groups were compared using one-way ANOVA and Tukey's post-hoc test. Differences in samples were considered significant if P is less than 0.05. P<0.05 (\*), P<0.01(\*\*), P<0.001(\*\*\*)

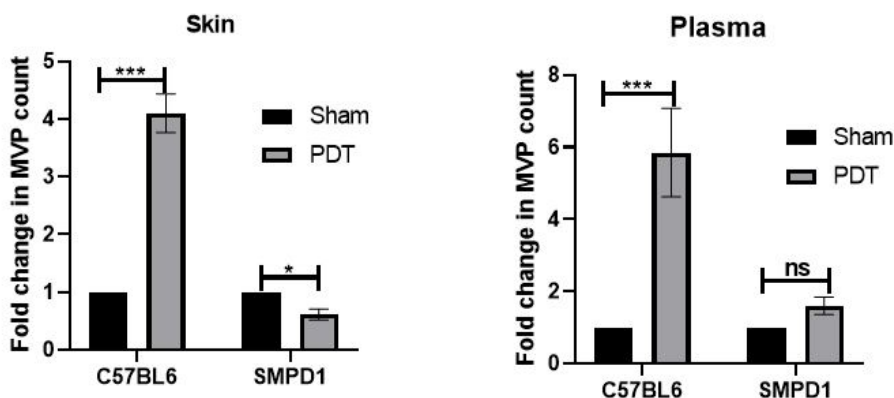


Figure 4.11: Role of acid sphingomyelinase in PDT-induced MVP release. C57BL6 and Smpd1 KO mice had their backs shaved and had PDT done as previously. There was no significant MVP generation following PDT in the Smpd1 KO mice unlike the C57BL6 strains. This further strongly suggests the major role aSMase plays in the generation of PDT-induced MVP. The data depicted are mean SD fold change in MVP count (n=4mice from a single experiment). Groups were compared using student's paired t-test. Differences in samples were considered significant if P is less than 0.05. P<0.05 (\*), P<0.01(\*\*), P<0.001(\*\*) and ns denotes not significant

## **4.4 Role of Platelet Activating Factor Receptor (PAFR) in PDT-generated MVP**

The platelet activating factor receptor (PAFR) has been implicated in the generation of MVPs following treatment with Ultraviolet B (UVB) [120]. As PDT is known to generate PAF, the next studies were thus designed to investigate the role of the PAFR in the generation of MVPs following PDT.

### **4.4.1 Role of PAFR in PDT-generated MVP *in vitro***

KB cells, derived from human nasopharyngeal cell line that do not express PAFR (designated as KBM cells) were employed to test the role of the receptor in the generation of MVPs following PDT. A part of these cells was transfected with the PAFR and designated as KBP cells. As shown in Fig.4.10, both KBP and KBM cells showed similar significant increase in the generation of MVPs. However, KBP cells responded to CPAF treatment by generating MVP unlike KBM cells. Moreover, both KBP and KBM cells responded to the PAF-independent stimulus PMA.

### **4.4.2 Role of PAFR in PDT-generated MVP *in vivo***

The next studies were defined to assess the role of PAF-R in PDT-mediated MVP generation in mice. *C57BL6* and *pafr* *-/-* mice had their backs shaved and were treated with PDT. Skin biopsies and plasma samples were taken after 4hrs. As shown in Fig.4.11, these studies revealed that MVP generation in both groups of mice was significantly increased following PDT as compared to the sham groups. However, PDT did not generate a significant increase in MVP on the *pafr* *KO* skin.

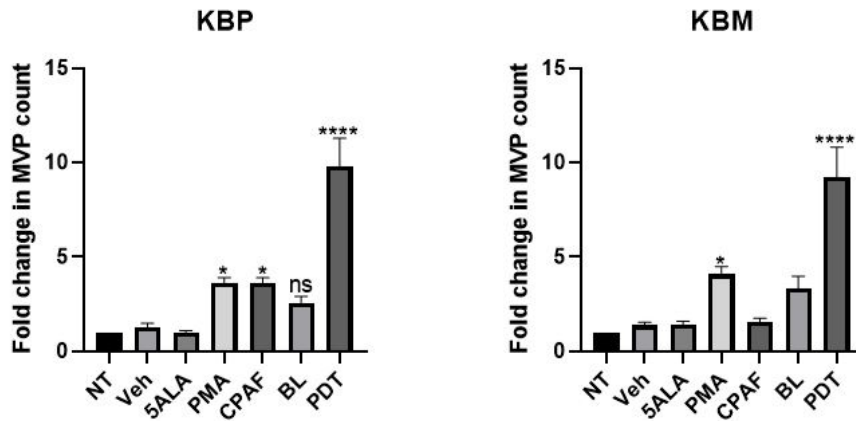


Figure 4.12: Role of PAFR in PDT-induced MVP generation using pafr +/- KB cells. PAFR-bearing KBP cells and PAFR negative KBM cells were treated with 100nm CPAF, 500nm PMA, PDT at 20J/cm<sup>2</sup> and incubated for 4hours before being processed for MVP isolation. PDT generated significant amount of MVP compared to the no treatment groups, suggesting a PAFR-independent process. The data depicted are mean SE fold change in MVP count (n=10). Groups were compared using one-way ANOVA and Tukey's post-hoc test. Differences in samples were considered significant if P is less than 0.05. P<0.05 (\*), P<0.0001(\*\*\*\*) and ns denotes not significant

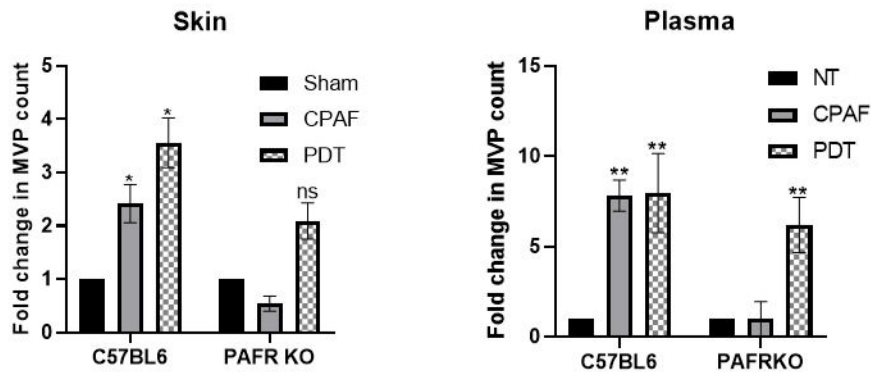


Figure 4.13: Role of PAFR in PDT-induced MVP. C57BL6 and pafr KO mice had their backs shaved and had PDT done as previously, with 250ng of CPAF. MVP generation in both groups of mice was significantly increased when compared to the sham groups. However, PDT did not generate a significant increase in MVP on the pafr KO skin. This could suggest a partial involvement of the PAFR in PDT-induced MVP generation. The data depicted are mean SD fold change in MVP count (n=6 mice). Groups were compared using one-way ANOVA and Tukey's post-hoc test. Differences in samples were considered significant if P is less than 0.05. P<0.05 (\*), P<0.01(\*\*) and ns denotes not significant.



# Discussion

## 5.1 Summary

PDT, despite its local application, is capable of generating systemic effects; some, which may be undesirable [76][48][38][86]. Mechanisms involved in this systemic response are poorly understood. Ferracini et al postulated that PAFR ligands play a role in the systemic immunosuppression observed following PDT [38]. Cytokines and certain inflammatory infiltrates have also been implicated in this effect [48][35]. PAFR ligands have been shown to be involved in the systemic immunosuppression caused by Ultraviolet B (UVB) exposure, as previously demonstrated by our lab [4]. This current study was designed to investigate the possible involvement of MVPs in PDT effects. MVPs, like other EVs, are believed to mediate certain cellular communications, act as potential biomarkers and can thus, mediate certain systemic effects in the body once generated. The present studies provide evidence that PDT can generate significant amounts of MVPs *in vitro*, *ex vivo* and *in vivo*. Although MVPs can be shed by all eukaryotic cell types, for this study we used keratinocytes- immortalized (HaCaT), modified (KBP/KBM), TERT-bearing (NTERT), and Fibroblasts. Our dose and time kinetic studies suggested 20J/cm<sup>2</sup> (1663s) and 4hrs post-blue light exposure as favorable and most efficient (Fig.4.1 and Fig.4.3). In furtherance to this, incubation with 5ALA for 4hrs followed by 20J/cm<sup>2</sup> (1663s) of blue light exposure produced the most lethal effect on HaCaT cells, being immortalized keratinocytes with tumorigenic abilities (Fig.4.2). The Federal Drug Administration (FDA) clinical guideline recommends 5-ALA

skin incubation for 14-18hrs, although 1-2hrs are commonly used in clinical practice [85]. Recent studies, however, suggests shorter 5ALA incubation times and lesser light exposure [62][13]. These variations could arise due to the different cells being used, and it is thus advisable, to adapt PDT conditions to suit each cell / tissue in focus. Normal human skin is capable of taking up ALA rapidly and converting it to porphyrin both *in vivo* and *ex vivo* [39]. Skin malignancies and pre-malignant conditions such as actinic keratoses, are thus not surprisingly very responsive to PDT likely through their ability to take up increased amounts of 5-ALA. Our model involved *ex vivo* (human skin) and *in vivo* (murine skin) investigation of PDT effect on skin and we observed a significant increase in MVP generation following PDT (Fig.4.4 and Fig.4.5). Circulating endogenous photosensitizers have been found to play some role in accelerated PDT response [59][51][64][112][58]. This agrees with the slight significance in the blue light alone treatment we observed in our study (Fig.4.4). Reactive Oxygen Species (ROS) generation is core to the effects of PDT and has been clearly explained to be its major mechanism of effecting tissue damage [100][81][16][108][99]. To validate the effects of this on MVP generation, we used the antioxidants Vitamin C (Vit C) and N-acetylcysteine (NAC). Both 0.5mM doses of Vit C and NAC acting alone sufficiently inhibited MVP generation following PDT. Their combination, however, did not yield any significant additive or synergistic effect (Fig.4.6). This is similar to several reports of attenuation of PDT effects in the presence of antioxidants [78][61][53][101]. Since generation of ROS is central to the actions of PDT, a corresponding inhibition in MVP production following the application of antioxidants as shown in our study, suggests the involvement of MVPs in PDT operations. The acid sphingomyelinase (aSMase) enzyme catalyses the reaction that leads to the formation of ceramide which in turn, causes MVP shedding off from the cell membrane. This forms the bedrock of MVP production from cells [24][27][92][87]. We validated aSMase involvement in PDT-generated MVP by using a potent inhibitor of the enzyme, Imipramine, and a murine model of the human Neimann-pick disease, *smpd1 KO* mice [55][1][96]. Imipramine significantly

inhibited the production of MVP following PDT *in vitro*, *ex vivo* and *in vivo* (Fig.4.7 and Fig.4.8). To further accentuate this, there was no significant generation of MVP in the *smpd1 KO* mice as compared to the wild type strains (Fig.4.9). This strongly agrees with the aSMase pathway being largely responsible for MVP production from cells. The G-coupled receptor, Platelet-activating factor receptor (PAFR) signaling has been shown to be involved in the release of MVP [70][120][106]. We envisaged its involvement in PDT-induced MVP generation and investigated using *in vitro* KB cells and *in vivo* *pafr KO* mice. Our *in vitro* studies showed that MVP generation in KB cells is independent on the PAFR (Fig.4.10). In furtherance to this, normal human Fibroblasts that have been shown to be deficient in PAFR [49][14], yielded significant amounts of MVP release following PDT treatment. Our *in vivo* data, however, suggests a partial involvement of PAFR as the MVP yield in *pafr KO* mice skin following, was insignificant as compared to the sham group. Further studies are needed to validate this. The model that is emerging appears to be that although PDT can generate PAFR agonists, and PAFR agonists generate MVP, yet PDT likely generates such a toxic stimulus to the cells that MVP are produced independently of the PAFR. Similar unpublished studies from our laboratory indicate that thermal burn injury can also induce MVP release in PAFR-negative KB cells. However, regarding thermal burn injury, consistently higher levels of MVP are generated in PAFR+ over PAFR-negative KB cells.

## 5.2 Limitations and Future Studies

Despite showing the generation of MVP following PDT and possible pathways involved, there is no strong evidence to validate the role MVPs play in the actions of PDT. As with other studies involving EVs, another limitation of this study is the difficulty in clearly delineating MVPs from smaller exosomes. As such, some exosomes may be involved in these actions attributed to MVPs. An important follow-up will be to investigate the up- and

downstream signaling involved in the generation of MVPs following PDT. Future studies could test the ability of imipramine to block PDT-induced cytokine/inflammatory effects in skin explants/mice. This could allow pharmacologic manipulation of the process to assess if MVP are involved in the inflammation or immunomodulation associated with PDT.

### **5.3 Conclusion**

These studies provide compelling evidence that PDT when used clinically results in the generation of MVPs. Thus, these studies suggest the possible involvement of MVP in the actions of PDT. An improved understanding of the exact role(s) of MVP in PDT clinical effectiveness/toxicities can result in novel strategies to improve this treatment modality. Thus, MVPs can be engineered to modify and widen the application of PDT. PDT-generated MVP release can be successfully blocked by imipramine and antioxidants. This can be possibly considered to help clinically to reduce side effects of PDT. The role of PAFR appears limited; further studies are needed.

# Appendix

## 6.1 Appendix 1: Supplemental Figures

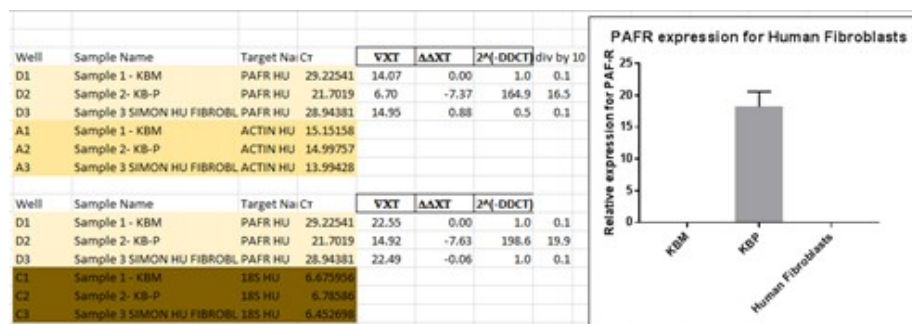


Figure 6.1: PAFR expression in KB cells and human fibroblasts. Total RNA was extracted from KB cells and Fibroblast by TRIzol and extracted RNA was quantified with Nanodrop One (thermo fisher). High-Capacity cDNA Reverse Transcription kit was used to transcribed RNA samples to cDNA for the analysis of the PAF-R mRNA expression using a SYBR green-based, quantitative fluorescent PCR method. The fluorescence was detected using a StepOne Real-Time PCR machine (Applied Biosystems, Foster City, CA, USA). Primers were specific for PAF-R, GAPDH (as an endogenous control) and PAF-R expression in these cell lines were compared with stably PAF-R-expressing cell line-KBP and PAF-R-deficient cell line-KBM as positive and negative controls. The quantification of each PCR product was normalized to GAPDH using the  $2^{-\Delta\Delta Ct}$  method.

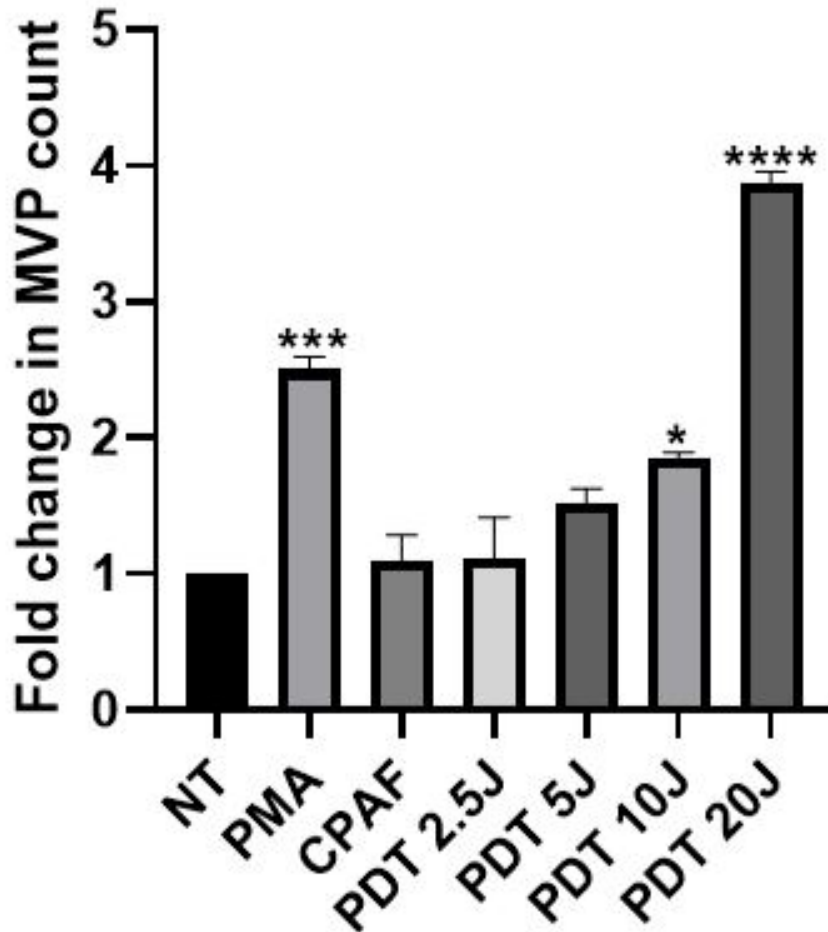


Figure 6.2: Dose response curve of PDT-induced MVP release in fibroblasts. Primary cultures of human fibroblasts either received No treatment (NT), 500ng PMA in 3ml HBSS+BSA, 100ng CPAF in 3ml HBSS+BSA, 2.5J PDT (208secs), 5J PDT (416secs), 10J PDT (832secs) or 20J PDT (1663secs). PMA and CPAF being positive and negative controls respectively. A progressive increase in MVP count was obtained as PDT dose increased, reaching a peak at 20J. The data depicted are mean + SE fold change in MVP count (average of n=2). Groups were compared using one-way ANOVA and Tukey's post-hoc test. Differences in samples were considered significant if the P value was less than 0.05. P<0.05 (\*), P<0.001(\*\*\*) and P<0.0001(\*\*\*\*).

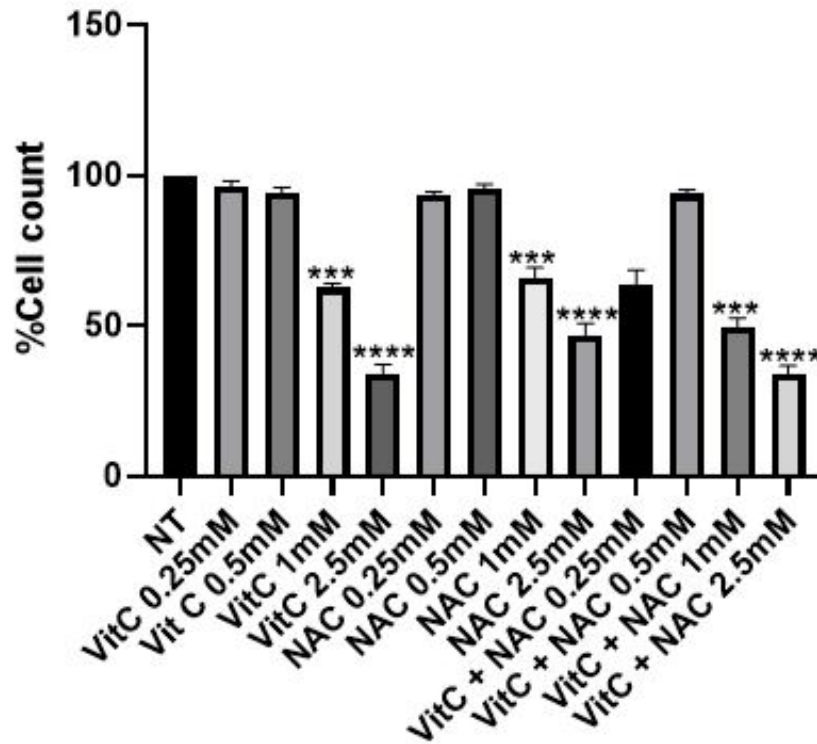


Figure 6.3: Relative survival rate of HaCaT cells following Antioxidant treatment. Ha-CaT cells had different concentrations of the antioxidants Vitamin C (VitC) and N-acetylcysteine (NAC) dissolved in fresh complete media and were incubated for 1hour at 37C. Plates subsequently had Trypan blue staining as described earlier and cell count was done with the Countess® machine. Cell count is taken as a percentage of the no treatment (NT) count. Higher doses of VitC and NAC significantly decreased cell count, appearing toxic. The data depicted are mean SE fold change in MVP count (average of n=3). Groups were compared using one-way ANOVA and Tukey's post-hoc test. Differences in samples were considered significant if P value is less than 0.05. P<0.001(\*\*\*) and P<0.0001(\*\*\*\*).

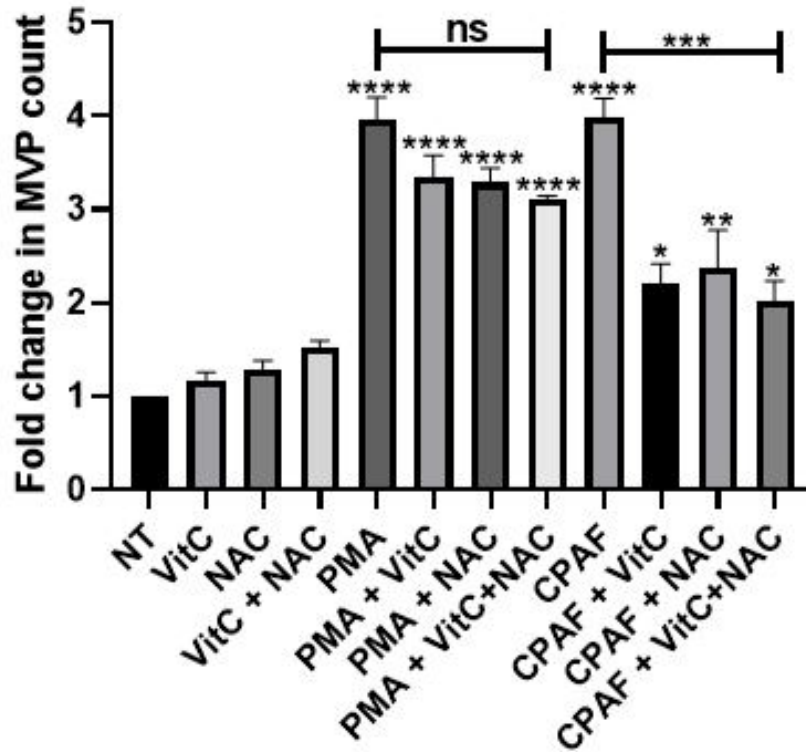


Figure 6.4: Effect of antioxidants on PMA- and CPAF-treated HaCaT cells. HaCaT cells were pre-treated with 0.5mM VitC and NAC for 1hour at 37C. They subsequently had 500ng PMA and 100ng CPAF both in 3ml HBSS+BSA treatments and were incubated for 4hours at 37C. Supernatants were harvested and processed for MVP isolation. Antioxidants reduced significantly the MVP generated by CPAF unlike PMA treated cells. The data depicted are mean SE fold change in MVP count (average of n=4). Groups were compared using one-way ANOVA and Tukey's post-hoc test. Differences in samples were considered significant if P value is less than 0.05. P<0.05(\*), P<0.01(\*\*), P<0.001(\*\*\*), P<0.0001(\*\*\*\*) and ns denotes not significant.



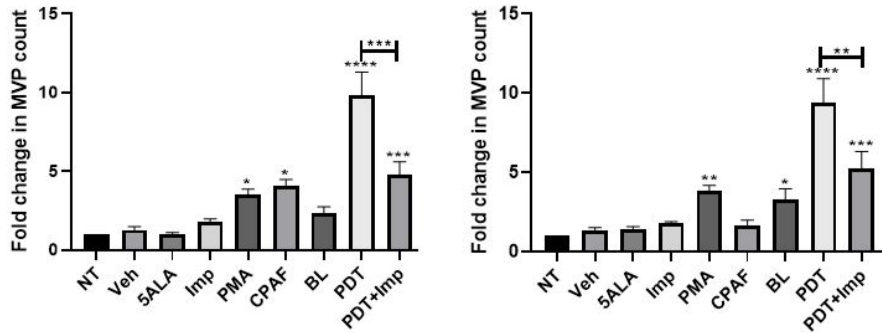


Figure 6.5: Imipramine inhibits production of MVPs by PDT in KB cells. KBP (a) and KBM (b) cells were treated with 50M imipramine, a known aSMase inhibitor, immediately after PDT. Other groups were treated with 100nm CPAF, 500nm PMA or 0.1%EtOH (Veh). Imipramine was able to inhibit production of MVPs by PDT significantly in these 2 cell lines. The data depicted are mean SE fold change in MVP count (average of n=8). Groups were compared using one-way ANOVA and Tukey's post-hoc test. Differences in samples were considered significant if P is less than 0.05. P<0.05 (\*), P<0.01(\*\*), P<0.001(\*\*\*), P<0.0001(\*\*\*\*).

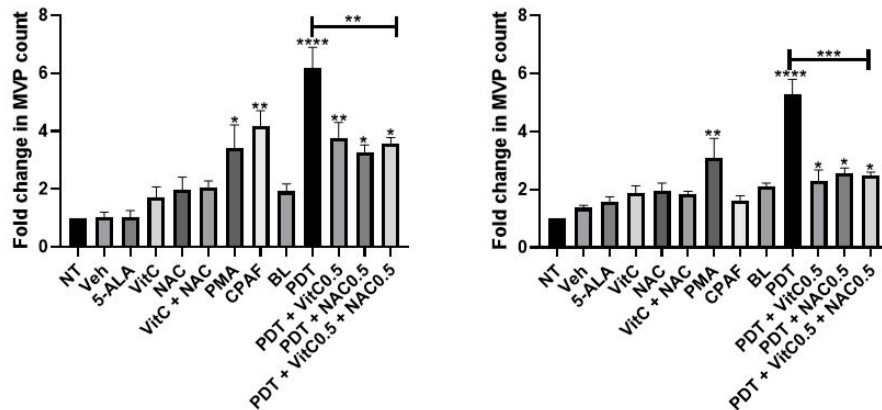


Figure 6.6: Antioxidants inhibits production of MVPs by PDT in KB cells. KBP (a) and KBM (b) cells had 5-ALA incubation in the dark for 4hrs and were then treated with the antioxidants, 0.5mM Vitamin C (VitC) and 0.5mM N-acetylcysteine (NAC) for 1hour. Cells were subsequently exposed to blue light and supernatant were harvested 4hrs later. Other groups were treated as earlier described. Both antioxidants significantly reduced MVP generated following PDT. There was, however, no difference when they were combined. The data depicted are mean SE fold change in MVP count (average of n=5). Groups were compared using one-way ANOVA and Tukey's post-hoc test. Differences in samples were considered significant if P is less than 0.05. P<0.05 (\*), P<0.01(\*\*), P<0.001(\*\*\*), P<0.0001(\*\*\*\*) and ns denotes not significant.

## 6.2 Appendix 2: Procedural Pictures

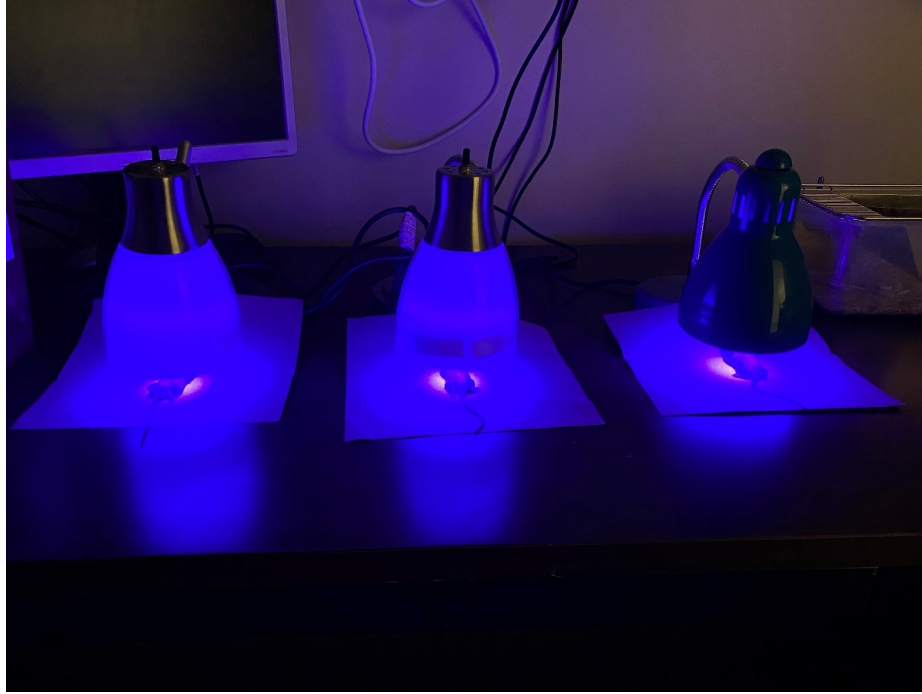


Figure 6.7: Groups of mice undergoing blue light treatment.



Figure 6.8: Skin preparation for PDT treatment.

# Bibliography

- [1] Smpd1 sphingomyelin phosphodiesterase 1, acid lysosomal [mus musculus (house mouse)]. *Gene - NCBI*.
- [2] Superoxide,  $o_2$ . *PubChem*.
- [3] Society i, vesicles e. minimal experimental requirements for definition of extracellular vesicles and their functions: a position statement from the international society for extracellular vesicles. 1:1–6, 2014.
- [4] Signaling pf. *HHS Public Access.*, 92(3):503–6, 2017.
- [5] Sudhakar A. History of cancer, ancient and modern treatment methods. *J Cancer Sci Ther.*, 1(2):1–4, 2009 Dec.
- [6] Uzdensky AB. The biophysical aspects of photodynamic therapy. *Biophys (Russian Fed.)*, 61(3):461–9, 2016 May 1.
- [7] Hamblin MR Abrahamse H. New photosensitizers for photodynamic therapy. *Biochem J.*, 473(4):347–64, 2016.
- [8] Kushner JP. Ajioka RS, Phillips JD. Biosynthesis of heme in mammals. *Med Princ Pract*, 1763:723–36, 2006.

- [9] Bonjour K Murphy RO Camacho V Ghiran I et al. Akuthota P, Carmo LAS. Extracellular microvesicle production by human eosinophils activated by “ inflammatory ” stimuli. 4:1–16, 2016 October.
- [10] Cuenca R Hu XH Childs CJH Sibata CH. Allison RR, Downie GH. Photosensitizers in clinical pdt. *Photodiagnosis Photodyn Ther*, 1(1):27–42, 2004 May.
- [11] Cerione RA. Antonyak MA, Wilson KF. *r(h)oads* to microvesicles. page 219–24, 2012 December.
- [12] Haberman HB. Aravind Menon I, Persad SD. A comparison of the phototoxicity of protoporphyrin, coproporphyrin and uroporphyrin using a cellular system in vitro. *Clin Biochem.*, 22(3):197–200, 1989 Jun.
- [13] Jagdeo J. Austin E. An in vitro approach to photodynamic therapy. *J Vis Exp*, 2018(138):3–8, 2018.
- [14] J. He; H.E. P. Bazan. Corneal myofibroblasts and keratocytes differ in paf–induced apoptosis. *Investigative Ophthalmology Visual Science*, Vol.45(1417):1417, May 2004.
- [15] Sandstrom PA Benov L. Buttke TM. Oxidative stress as a mediator of apoptosis. *Immunol Today*, 15(1):7–10, 1994.
- [16] Dondi A Cervellati C. Bergamini C, Gambetti S. Oxygen, reactive oxygen species and tissue damage. *Curr Pharm Des.*, 10(14):1611–26, 2005 Mar 18.
- [17] Rifkind AB Harber LC Kappas A. Bickers DR, Keogh L. Studies in porphyria. vi. biosynthesis of porphyrins in mammalian skin and in the skin of porphyric patients. *J Invest Dermatol.*, 68(1):5–9, 1977 Jan.

- [18] Chen Y Travers JB. Bihl JC, Rapp CM. Uvb generates microvesicle particle release in part due to platelet-activating factor signaling. *Photochem Photobiol*, 92(3):503–6, 2016 May 1.
- [19] Mahoney MJ. Bloomer JR, Brenner DA. Study of factors causing excess protoporphyrin accumulation in cultured skin fibroblasts from patients with protoporphyria. *J Clin Invest.*, 60(6):1354–61, 1977.
- [20] Llorente A Lo J Revento J Portillo HA et al. Buzas EI, Manc M. Biological properties of extracellular vesicles and their physiological functions. 1:1–60, 2015.
- [21] Hudson EJ Ash D V. Brown SB. Cairnduff F, Stringer MR. Superficial photodynamic therapy with topical 5-aminolaevulinic acid for superficial primary and secondary skin cancer. *Br J Cancer*, 69(3):605–8, 1994.
- [22] Laurenzana I Trino S Luca L De Lamorte D et al. Caivano A, Rocca F La. Extracellular vesicles in hematological malignancies: From biology to therapy.
- [23] Hamblin M. Castano AP, Demidova TN. Mechanisms in photodynamic therapy: part one. *Photodiagnosis Photodyn Ther.*, 1(4):279–93, 2004.
- [24] O’Driscoll L. Catalano M. Inhibiting extracellular vesicles formation and release: a review of ev inhibitors. *J Extracell Vesicles*, 9(1), 2020.
- [25] Webb RC. Chiao CW, Tostes RC. *p2x7* receptor activation amplifies lipopolysaccharide-induced vascular hyporeactivity via *interleukin – 1b* release. *J Pharmacol Exp Ther.*, 326(3):864–70, 2008 Sep.
- [26] Parker S Shahabi S Bahador A. Chiniforush N, Pourhajibagher M. The in vitro effect of antimicrobial photodynamic therapy with indocyanine green on enterococcus faecalis: Influence of a washing vs non-washing procedure. *Photodiagnosis Photodyn Ther*, 16:119–23, 2016.

- [27] Nigro A Podini P Finardi A Casella G et al. Colombo F, Bastoni M. Cytokines stimulate the release of microvesicles from myeloid cells independently from the p2x7 receptor/acid sphingomyelinase pathway. *Front Immunol.*, 9, 2018 Feb.
- [28] Foote CS. Definition of type i and type ii photosensitized oxidation. *Photochemistry and Photobiology.*, Vol. 54:p. 659–659., 1991.
- [29] Bjerring P Martino Neumann HA. De Leeuw J, Van Der Beek N. Photodynamic therapy of acne vulgaris using 5 – aminolevulinic acid 0.5% liposomal spray and intense pulsed light in combination with topical keratolytic agents. *J Eur Acad Dermatology Venereol*, 24(4):460–9, 2010 Apr.
- [30] Ino Y Ronfard V Wu JY Weinberg RA et al. Dickson MA, Hahn WC. Human keratinocytes that express htert and also bypass a *p16ink4a – enforced* mechanism that limits life span become immortal yet retain normal growth and differentiation characteristics. *Mol Cell Biol*, 20(4):1436–47, 2000 Feb 15.
- [31] Terra LF Baptista MS Labriola L. Dos Santos AF, De Almeida DRQ. Photodynamic therapy in cancer treatment - an update review. *J Cancer Metastasis Treat.* 2019, 2019.
- [32] Henderson BW Jori G Kessel D Korbek M et al. Dougherty TJ, Gomer CJ. Photodynamic therapy. *Thomas. J Natl Cancer Inst*, 90(12):889–905, 1998.
- [33] Valenzano DP. Photomodification of biological membranes with emphasis on singlet oxygen mechanisms. *Photochemistry and Photobiology*, Vol. 46:p. 147–60, 1987.
- [34] Souza Salvador SL de Bagnato VS Oliveira Junior OB de Esteban Florez FL, Gabriel Del Arco MC. Viability study of antimicrobial photodynamic therapy using curcumin, hypericin and photogem photosensitizers in planktonic cells of streptococcus mutans. *Sci J Dent*, 2:22–7, 2015.



- [35] White RD Sorefan NB Wright KP McLean K et al. Evangelou G, Farrar MD. Topical aminolaevulinic acid-photodynamic therapy produces an inflammatory infiltrate but reduces langerhans cells in healthy human skin in vivo. *Br J Dermatol.*, 165(3):513–9, 2011.
- [36] Fang JC Zhang L Diego S Jolla L. Fang RH, Jiang Y. *HHS Public Access.*, page 69–83, 2018.
- [37] Pignatari GC Evangelinellis MM Tavolari S Muotri AR et al. Fernandes IR, Russo FB. Fibroblast sources: Where can we get them? *Cytotechnology*, 68(2):223–8, 2016 Mar 1.
- [38] Harrison KA Waeiss RA Murphy RC Jancar S et al. Ferracini M, Sahu RP. Topical photodynamic therapy induces systemic immunosuppression via generation of platelet-activating factor receptor ligands. *J Invest Dermatol.*, 135(1):321–3, 2015.
- [39] Bolsen K Schulte KW Zumdick M Ruzicka T et al. Fritsch C, Batz J. Ex vivo application of -aminolevulinic acid induces high and specific porphyrin levels in human skin tumors: Possible basis for selective photodynamic therapy. *Photochem Photobiol.*, 66(1):114–8., 1997.
- [40] Goetz AE Stahl W Bolsen K Ruzicka T et al. Fritsch C, Abels C. Porphyrins preferentially accumulate in a melanoma following intravenous injection of 5-aminolevulinic acid. *Biol Chem.*, 378(1):51–7, 1997.
- [41] Schulte K-W Neuse WHG Ruzicka T Lehmann P. Fritsch C, Lang K. Fluorescence diagnosis with –aminolevulinic acid-induced porphyrins in dermatology. In: *Dermatological Phototherapy and Photodiagnostic Methods. Springer Berlin Heidelberg*, page p. 344–67, 2001.
- [42] Burnstock G. *p2x* ion channel receptors and inflammation. *Purinergic Signal*, 12(1):59–67, 2016 Mar 1.



- [43] Sellera DP Fregnani ER. Garcez AS, Arantes-Neto JG. Effects of antimicrobial photodynamic therapy and surgical endodontic treatment on the bacterial load reduction and periapical lesion healing. three years follow up. *Photodiagnosis Photodyn Ther*, 12(4):575–80, 2015.
- [44] Bolsen K Zumdick M Fritsch C Schurer NY. Goerz G, Link-Mannhardt A. Porphyrin concentrations in various human tissues. *Exp Dermatol.*, 4(4 Pt 1):218–20, 1995 Aug.
- [45] Buettner GR. The pecking order of free radicals and antioxidants: Lipid peroxidation, -tocopherol, and ascorbate. *Arch Biochem Biophys.*, 300(2):535–43., 1993.
- [46] Malik Z. Hanania J. The effect of edta and serum on endogenous porphyrin accumulation and photodynamic sensitization of human k562 leukemic cells. *Cancer Lett.*, 65(2):127–31., 1992 Aug.
- [47] Neill SJ. Hancock JT, Desikan R. Cytochrome c, glutathione, and the possible role of redox potentials in apoptosis. *Annals of the New York Academy of Sciences. New York Academy of Sciences*, page p. 446–8, 2003.
- [48] Sugihara A Horio T. Hayami J, Okamoto H. Immunosuppressive effects of photodynamic therapy by topical aminolevulinic acid. *J Dermatol.*, 34(5):320–7, 2007.
- [49] Bazan HEP. He J. Synergistic effect of platelet-activating factor and tumor necrosis factor- on corneal myofibroblast apoptosis. *Investig Ophthalmol Vis Sci.*, 47(3):883–91, 2006 Mar 1.
- [50] Cai H. Hu C. Application of photodynamic fluorescence diagnosis in skin tumors. in: Luo q, li x, gu y, tang y, editors. optics in health care and biomedical optics viii. *SPIE*, page p. 162–71., 2018.

- [51] Zhiyentayev T Sharma SK Balasubramanian T Ruzié C et al. Huang YY, Mroz P. In vitro photodynamic therapy and quantitative structure-activity relationship studies with stable synthetic near-infrared-absorbing bacteriochlorin photosensitizers. *J Med Chem.*, 53(10):4018–27, 2010 May 27.
- [52] Hazama H Akter S Fuse S Nakamura H et al Inai M, Honda N. Photodynamic therapy using a cytotoxic photosensitizer porphyrus envelope that targets the cell membrane. *Photodiagnosis Photodyn Ther*, 20:238–45, 2017 August.
- [53] Farkas O. Jakus J. Photosensitizers and antioxidants: A way to new drugs? *Photochemical and Photobiological Sciences. The Royal Society of Chemistry*, page p. 694–8., 2005.
- [54] Travers JB. Oxidative stress can activate the epidermal platelet-activating factor receptor. *J Invest Dermatol*, 112(3):279–83, 1999 Mar.
- [55] Katouzian F Darroch PI Schuchman EH. Jones I, He X. Characterization of common smpd1 mutations causing types a and b niemann-pick disease and generation of mutation-specific mouse models. *Mol Genet Metab*, 95(3):152–62, 2008 Nov.
- [56] Soncin M Ferro S Coppellotti O Dei D et al. Jori G, Fabris C. Photodynamic therapy in the treatment of microbial infections: Basic principles and perspective applications. *lasers surg med. Med Princ Pract*, 38(5):468–81, 2006 Jun.
- [57] Drobizhev M Rebane A Nickel E Spangler CW. Karotki A, Kruk M. Efficient singlet oxygen generation upon two-photon excitation of new porphyrin with enhanced nonlinear absorption. *IEEE J Sel Top Quantum Electron.*, 7(6):971–5, 2001 Nov.
- [58] Pottier RH. Kennedy JC, Marcus SL. Photodynamic therapy (pdt) and photodiagnosis (pd) using endogenous photosensitization induced by (ala): Mechanisms and clinical results. *J Clin Laser Med Surg.*, 14(5):289–304, 1996 Oct.

- [59] Pross DC. Kennedy JC, Pottier RH. Photodynamic therapy with endogenous protoporphyrin ix: basic principles and present clinical experience. *J Photochem Photobiol B.*, 6(1–2):143–8, 1990 Jun.
- [60] Gasser S. Khan M. Generating primary fibroblast cultures from mouse ear and tail tissues. *J Vis Exp.*, 2016(107), 2016 Jan 10.
- [61] Bruce JI MacRobert AJ Golding JP. Kimani SG, Phillips JB. Antioxidant inhibitors potentiate the cytotoxicity of photodynamic therapy. *Photochem Photobiol.*, 88(1):175–87, 2012 Jan.
- [62] Mamalis A Jagdeo J. Koo E, Austin E. Efficacy of ultra short sub-30 minute incubation of 5 – *aminolevulinic* acid photodynamic therapy in vitro. *Lasers Surg Med.*, 49(6):592–8, 2017.
- [63] Mamalis A Jagdeo J. Koo E, Austin E. Thermal ultra short photodynamic therapy: Heating fibroblasts during sub 30-minute incubation of 5 – *aminolevulinic* acid increases photodynamic therapy induced cell death. *Dermatologic Surg*, 44(4):528–33, 2018 Apr 1.
- [64] Yang L. Kou J, Dou D. Porphyrin photosensitizers in photodynamic therapy and its applications. *Oncotarget. Impact Journals LLC*, Vol. 8(24(suppl 1)):p. 81591–603., 2017.
- [65] Benov L. Photodynamic therapy: Current status and future directions. *Med Princ Pract*, (24(suppl 1)):14–28, 2015.
- [66] Yellon DM Davidson SM. Lawson C, Vicencio JM. Microvesicles and exosomes: new players in metabolic and cardiovascular disease. 2016.
- [67] Jon Williams K Liu ML. Li M, Yu D. Tobacco smoke induces the generation of pro-

coagulant microvesicles from human monocytes/macrophages. *Arterioscler Thromb Vasc Biol.*, 30(9):1818–24, 2010 Sep.

- [68] Ross RA Zhao Z Xu Y Crabb DW. Liangpunsakul S, Rahmini Y. Imipramine blocks ethanol-induced aspmase activation, ceramide generation, and *pp2a* activation, and ameliorates hepatic steatosis in ethanol-fed mice. *Am J Physiol - Gastrointest Liver Physiol*, 302(5):G515–23, 2012 Mar 1.
- [69] He D. Lim HW, Behar S. Effect of porphyrin and irradiation on heme biosynthetic pathway in endothelial cells. *Photodermatol Photoimmunol Photomed.*, 10(1):17–21, 1994 Feb.
- [70] Rapp C Romer E Borchers C Bihl J et al Liu L, Fahy K. Uvb induces mvp release in a paf dependent manner in skin-derived epithelial cell line. *Pharmacol Toxicol Fac Publ*, 2017 May 10.
- [71] Tedgui A Boulanger CM. Loyer X, Vion AC. Microvesicles as cell-cell messengers in cardiovascular diseases. *Circulation Research. Lippincott Williams and Wilkins*, Vol. 114:p. 345–53, 2014.
- [72] Kornek M. Large extracellular vesicles: Have we found the holy grail of inflammation? 9:1–22, 2018 9(December).
- [73] Ochsner M. Photophysical and photobiological processes in the photodynamic therapy of tumours. *J Photochem Photobiol B.*, 39(1):1–18, 1997 May.
- [74] Varol M. An alternative treatment modality of diseases using photodynamic therapy with a wide range biological targeting possibility. 3(4):21–5, 2015.
- [75] Jori G Abels C. Maisch T, Szeimies RM. Antibacterial photodynamic therapy in dermatology. *Photochemical and Photobiological Sciences.*, Vol. 3:p. 907–17, 2004.

- [76] Damian DL, Matthews YJ. Topical photodynamic therapy is immunosuppressive in humans. *Br J Dermatol.*, 162(3):637–41, 2010.
- [77] MacKay JA, Evans WK, Maziak DE, Markman BR. Photodynamic therapy in non-small cell lung cancer: A systematic review. *Ann Thorac Surg.*, 77(4):1484–91, 2004.
- [78] Belitchenko I, Potapenko AY, Merlin J-L, Guillemin FH, Melnikova V, Bezdetyayna LN. Effect of antioxidants on pdt treatment of cultured tumor cells; in: Dougherty tj, editor. optical methods for tumor treatment and detections: Mechanisms and techniques in photodynamic therapy vii. *SPIE*, page p. 145–9, 1998.
- [79] Arshad H, Mimikos C, Shafirstein G. Current state and future of photodynamic therapy for the treatment of head and neck squamous cell carcinoma. *World J Otorhinolaryngol Neck Surg [Internet].*, 2(2):126–9, 2016.
- [80] Bagdonas S, Bech O, Berg K, Moan J, Streckyte G. Photobleaching of protoporphyrin ix in cells incubated with 5 – aminolevulinic acid. *Int J cancer*, 70(1):90–7, 1997 Jan 6.
- [81] Ivan MT, Heidi A, Mokwena MG, Kruger CA. A review of nanoparticle photosensitizer drug delivery uptake systems for photodynamic treatment of lung cancer. *Photodiagnosis Photodyn Ther [Internet].*, page 147–54, 2018;22(February).
- [82] Plou C, Romao M, Chavrier P, Raposo G et al. Muralidharan-Chari V, Clancy J. *arf6 – regulated* shedding of tumor cell-derived plasma membrane microvesicles. *Curr Biol*, 19(22):1875–85, 2009 Dec 1.
- [83] Fusenig NE. Normal keratinization in a spontaneously immortalized. 106:761–71, 1988 March.

- [84] Calzavara-Pinton P, Ortel B. Advances in photodynamic therapy. a review. *G Ital Dermatol Venereol.*, 145(4):461–75, 2010 Aug.
- [85] Fabi SG, Gold MH, Goldman MP, Lowe NJ et al. Ozog DM, Rkein AM. Photodynamic therapy: A clinical consensus guide. *Dermatologic Surgery. Lippincott Williams and Wilkins*, Vol. 42:p. 804–27, 2016.
- [86] Murphy RC, Johnson CA, Kelley SW, Dy LC et al. Pei Y, Barber LA. Activation of the epidermal platelet-activating factor receptor results in cytokine and cyclooxygenase – 2 biosynthesis. *J Immunol*, 161(4):1954–61, 1998.
- [87] Lanuti P, Ercolino E, Di Ioia M, Zucchelli M et al. Pieragostino D, Cicalini I. Enhanced release of acid sphingomyelinase-enriched exosomes generates a lipidomics signature in csf of multiple sclerosis patients. *Sci Rep.*, 8(1), 2018 Dec 1.
- [88] Berlanda J, Berr F, Kiesslich T, Plaetzer K, Krammer B. Photophysics and photochemistry of photodynamic therapy: Fundamental aspects. *Lasers Med Sci.*, (24(2)):259–268, 2009.
- [89] Prasad PN. Introduction to biophotonics. *John Wiley Sons, Inc.*, 2003.
- [90] Bo AN, Pol E, Van Der. Classification, functions, and clinical relevance of extracellular vesicles. 64(3):676–705, 2012.
- [91] Stafforini DM, McIntyre TM, Prescott SM, Zimmerman GA. Platelet-activating factor and related lipid mediators. *Annu Rev Biochem.*, 69:419–45., 2000.
- [92] Poirot M, Wakelam MJO, Record M, Silvente-Poirot S. Extracellular vesicles: Lipids as key components of their biogenesis and functions. *J Lipid Res.*, 59(8):1316–24., 2018.

- [93] Menser MB Aires DJ Schweiger ES Riddle CC, Terrell SN. A review of photodynamic therapy (pdt) for the treatment of acne vulgaris. *J Drugs Dermatol*, 8(11):1010–9, 2009 Nov.
- [94] Weyerbacher J Murphy RC Konger RL Garrett JE et al. Sahu RP, Harrison KA. Radiation therapy generates platelet-activating factor agonists. *Oncotarget*, 7(15):20788–800, 2016 Apr 12.
- [95] Buettner GR. Schafer FQ. Redox environment of the cell as viewed through the redox state of the glutathione disulfide/glutathione couple. *Free Radical Biology and Medicine.*, Vol. 30:p. 1191–212, 2001.
- [96] Hibbert SR Sawitsky A Brady RO. Schneider EL, Pentchev PG. A new form of niemann-pick disease characterised by temperature-labile sphingomyelinase. *J Med Genet.*, 15(5):370–4, 1978.
- [97] Fusenig NE. Schoop VM, Mirancea N. Epidermal organization and differentiation of hacat keratinocytes in organotypic coculture with human dermal fibroblasts. *J Invest Dermatol*, 112(3):343–53, 1999 Mar.
- [98] Harris K Baumann H Gollnick SO Lindenmann J et al. Shafirstein G, Battoo A. Photodynamic therapy of non-small cell lung cancer narrative review and future directions. *Ann Am Thorac Soc.*, 13(2):265–75., 2016.
- [99] Gao J Wang Z. Shi X, Zhang CY. Recent advances in photodynamic therapy for cancer and infectious diseases. *Wiley Interdiscip Rev Nanomedicine Nanobiotechnology*, 11(5):1–23, 2019.
- [100] Kohl EA Karrer S Landthaler M Szeimies RM. Steinbauer JM, Schreml S. Die photodynamische therapie in der dermatologie. *JDDG - J Ger Soc Dermatology.*, 8(6):454–66, 2010.

- [101] Wei Y Yin L. Sun D, Zhang S. Antioxidant activity of mangostin in cell-free system and its effect on k562 leukemia cell line in photodynamic therapy. *Acta Biochim Biophys Sin (Shanghai)*, 41(12):1033–43, 2009.
- [102] Karrer S. Szeimies R-M, Landthaler M. Non-oncologic indications for ala-pdt. *J Dermatolog Treat.*, 13 Suppl 1:S13–8, 2002.
- [103] Ito T. Cellular and subcellular mechanisms of photodynamic action: The  $o_2$  hypothesis as a driving force in recent research. *Photochem Photobiol*, 28(4–5):493–506, 1978.
- [104] Dixon SJ. Tarangelo A. Nanomedicine: An iron age for cancer therapy. *Nature Nanotechnology*. Nature Publishing Group, Vol. 11:p. 921–2., 2016.
- [105] Brown SB. Taylor EL. The advantages of aminolevulinic acid photodynamic therapy in dermatology. *J Dermatolog Treat.*, 13 Suppl 1::S3–11, 2002.
- [106] Liu L Kelly LE Rapp CM Chen Y et al. Thyagarajan A, Kadam SM. Gemcitabine induces microvesicle particle release in a platelet-activating factor-receptor-dependent manner via modulation of the mapk pathway in pancreatic cancer cells. *Int J Mol Sci.*, 20(1), 2019.
- [107] Aikawa E Alcaraz MJ Anderson JD Andriantsitohaina R et al. Théry C, Witwer KW. Minimal information for studies of extracellular vesicles 2018 (*misev2018*): a position statement of the international society for extracellular vesicles and update of the misev2014 guidelines. page 7, 2018.
- [108] Huang P. Trachootham D, Alexandre J. Targeting cancer cells by ros-mediated mechanisms: A radical therapeutic approach? *Nature Reviews Drug Discovery.*, Vol. 8:p. 579–91., 2009.



- [109] Mang TS. Lasers and light sources for PDT: Past, present and future. *Photodiagnosis Photodyn Ther.*, 1(1):43–8, 2004 May 1.
- [110] Azinovic I, Rebollo J, Canon R, Sapena NS et al. Vanaclocha V, Sureda M. Photodynamic therapy in the treatment of brain tumours: a feasibility study. *Photodiagnosis Photodyn Ther.*, 12(3):422–7, 2015.
- [111] Ma X, Cheng C, Xiao X, Chen J et al. Wang J, Chen S. Effects of endothelial progenitor cell-derived microvesicles on hypoxia/reoxygenation-induced endothelial dysfunction and apoptosis. *Oxid Med Cell Longev.*, 2013:572729, 2013.
- [112] Fromm D, Webber J, Kessel D. Photodynamic therapy using endogenous photosensitization for gastrointestinal tumors. *Yale J Biol Med.*, 70(1):127–37, 1997.
- [113] Editors G, Mause SF, Weber C, Weber C, Mause S. Protagonists of a novel communication network for intercellular information exchange. page 1047–57, 2010.
- [114] Dougherty TJ, Weishaupt KR, Gomer CJ. Identification of singlet oxygen as the cytotoxic agent in photo inactivation of a murine tumor. *Cancer Res.*, 36(7), 1976.
- [115] Na R, Wulf HC, Wiegell SR, Stender IM. Pain associated with photodynamic therapy using 5-aminolevulinic acid or 5-aminolevulinic acid methylester on tape-stripped normal skin. *Arch Dermatol.*, 139(9):1173–7, 2003 Sept 1.
- [116] Kerl H, Wolf P, Rieger E. Topical photodynamic therapy with endogenous porphyrins after application of 5-aminolevulinic acid: an alternative treatment modality for solar keratoses, superficial squamous cell carcinomas, and basal cell carcinomas? *J Am Acad Dermatol.*, 28(1):17–21, 1993 Jan.
- [117] Liu L, Wang J, Bi K, Liu Y et al. Xiao X, Ma X. Cellular membrane microparticles: Potential targets of combinational therapy for vascular disease. *Curr Vasc Pharmacol.*, 13(4):449–58, 2015 Aug 4.

- [118] Obata M Hagiya Y Ogura S ichiro Ikeda A et al. Yano S, Hirohara S. Current states and future views in photodynamic therapy. *J Photochem Photobiol C Photochem Rev [Internet].*, 12(1):46–67, 2011.
- [119] Al-Hassani M Murphy RC Rezaia S Konger RL et al. Yao Y, Harrison KA. Platelet-activating factor receptor agonists mediate xeroderma pigmentosum a photosensitivity. *J Biol Chem.*, 287(12):9311–21, 2012 Mar 16.
- [120] Zhang Q Marathe GK Al-Hassani M Konger RL et al. Yao Y, Wolverson JE. Ultraviolet b radiation generated platelet-activating factor receptor agonist formation involves egf-r-mediated reactive oxygen species. *J Immunol.*, 182(5):2842–8, 2009.

